Published by Avanti Publishers

Journal of Chemical Engineering Research Updates

ISSN (online): 2409-983X

Synthesis and Potential Applications of Modified Xanthan Gum

Mahmoud H. Abu Elella*

Chemistry Department, Faculty of Science, Cairo University, Giza 12613, Egypt.

ARTICLE INFO

Article Type: Research Article

Keywords:
Xanthan gum
Protein delivery
Wastewater treatment
Biomedical application
Antibacterial materials

Timeline:
Received: September 29, 2021
Accepted: November 26, 2021
Published: December 27, 2021

Citation: Abu Elella MH. Synthesis and Potential Applications of Modified Xanthan Gum. J Chem Eng Res Updates, 2021; 8: 73-97.

DOI: https://doi.org/10.15377/2409-983X.2021.08.6

ABSTRACT

Designing high-performance adsorbents for wastewater treatment and antibacterial materials for food and biomedical applications and excellent drug carrier to prolong time retention of the therapeutic drug based on biodegradable polymers has gained more interest in recent years. Among these materials, xanthan gum, which is a natural polysaccharide and plays a vital role in various applications such as industry, enhanced oil recovery, water-based paints, pharmaceuticals, and personal care products because it has excellent properties such as biodegradability and non-toxicity. On the other hand, it has many affected limitations, including microbially attack, poor thermal and mechanical stability, and low surface area. So, in this review, we focused on the advanced modifications on xanthan gum and their applications in wastewater treatment, protein delivery, and designing antimicrobial materials.

*Corresponding Author
Email: mahmoudhussien3766@yahoo.com
Tel: +2001207119559

1. Introduction

Polymeric materials are considered nowadays as an important class of materials in diversified fields than conventional materials due to their physicochemical properties [1]. A polymer is a macromolecule composed of small repeating units (monomers) joined together through covalent bonds. According to the origin of polymer, it is either natural (if it is produced from natural sources such as plants, animals, and microorganisms) or synthetic [2, 3]. Natural polymers have many advantages over synthetic polymers, such as high availability (low cost), easy processing, biocompatible, biodegradable, non-toxic, and eco-friendly [2, 4, 5].

2. Polysaccharides

Polysaccharides are an example of natural polymers composed of carbohydrate structure with a large polymeric oligosaccharide formed through glycosidic linkages between multiple monosaccharides as repeating units [6, 7]. Polysaccharides are the most abundant organic compounds in nature due to their natural origins. They can be extracted from renewable resources such as plants (e.g., starch, cellulose), animals (e.g., chitin, hyaluronic acid), and micro- organisms (e.g., xanthan gum, gellan gum) [4, 6, 8-13].

Polysaccharides are classified into two categories; homopolysaccharides and heteropolysaccharides. Homopolysaccharides are composed of the same mono-saccharides as repeating units as starch, cellulose, glycogen, and pectin. In contrast, heteropolysaccharides are composed of different monosaccharides as repeating units, including xanthan gum, hyaluronic acid, etc. [6, 14-17].

In addition, polysaccharides have been applied in different applications due to their fabulous properties: availability at less cost, amenability to modifications, easy manufacture, good biocompatibility, and biodegradability in addition to non-toxicity, good solubility in water, and bioactive [4, 6, 18-20].

In the USA, the annual industrial consumption of polysaccharides is about 3 X 10^9 Kg (the market value of three trillion dollars) [21, 22]. Xanthan gum is one of the polysaccharides employed in various industrial applications [23, 24].

2.1. Xanthan Gum

2.1.1. History

In the 1950s, Allene Jeanes and co-workers discovered xanthan gum (XG) at the research center of the United States Department of Agriculture (USDA) during a program studying bacterial biopolymer production. Interestingly, the high molecular weight of xanthan gum was firstly extracted from *Xanthomonas campestris* NRRL B-1459. The first industrial production of XG was achieved in 1960, and then it was available as a commercial product in 1964 [4, 25-28]. XG is the second exo-polysaccharide after dextran, which was discovered in the early 1940s [4].

XG is a non-toxic compound, so it does not cause skin or eye irritation. Moreover, in 1969, XG was approved by the US Food and Drug Administration (FDA) as a safe food additive (stabilizer and emulsifier) and using it in food products with any quantity (without any limitation). Also, XG is registered in the Code of Federal Regulations (CFR) as a stabilizer and thickener agent. Furthermore, XG was approved by the European Commission (EC) under the number E415 in the permitted stabilizers, and thickeners list in 1980[25, 29-32]. The acceptable daily intake of XG was changed to a non-quantitative limit “not specified,” so it confirmed the XG status as a safe food additive[25].

2.1.2. Structure

XG is a natural anionic exo-polysaccharide with a high molecular weight. In 1975, the primary structure of XG was established; it includes five repeating units such as two glucose unites, two mannose unites, and one unit of glucuronic acid. The backbone of XG is similar to the cellulose structure. Its branched-chain contains terminal β-D-mannose that is linked via β-(1-4) to D-glucuronic acid, which is linked via α-(1-2) to D-mannose (Fig. **1**) [4, 33-37]. D-mannose units in XG are attached by pyruvate and acetate groups depending on microbial strain type [35,38-40].

While the secondary structure of XG appears as a five-fold helical structure with a pitch of 4.7 nm and a diameter of 1.9 nm that is stabilized by a non-covalent bond. The reversible order-disorder conformational transition of the secondary structure of XG can be induced by altering the temperatures and/or the ionic strength. Thus the disorder form is favored by high temperatures and low salt concentrations [4, 25, 35, 41-43].

Xanthan gum contains a large distributed molecular weight range (> 1 million $gmol^{-1}$). It depends on both the association between chains, forming aggregates of several individual chains, and the variations of the fermentation conditions [28, 44].

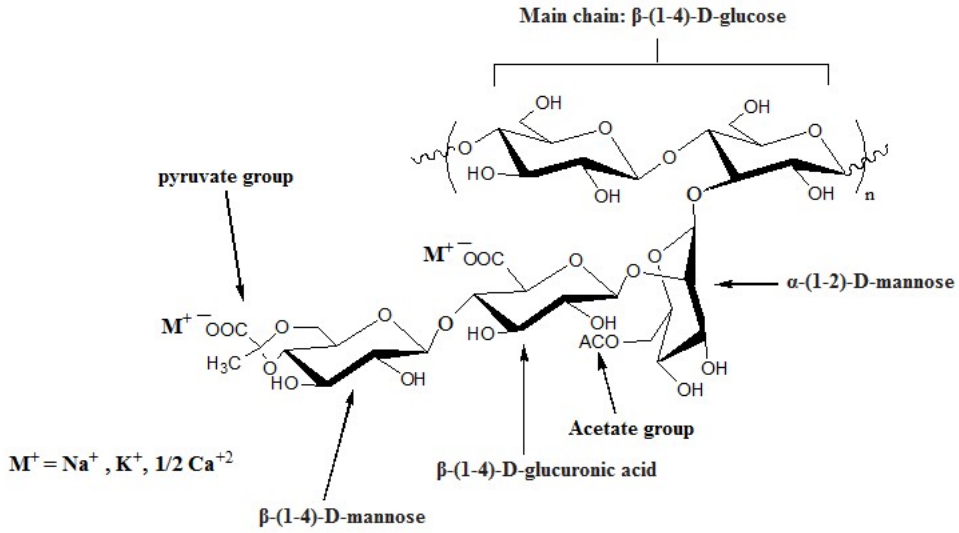

Figure 1: The chemical structure of Xanthan gum.

2.1.3. Production of XG

XG is produced from many *Xanthomonas spp*. such as *Xanthomonas campestris, Xanthomonas pelargonii, Xanthomonas phaseoli* and *Xanthomonas malvacearum* through aerobic fermentation [30, 45-47].

The production of XG depends on microbial species at an industrial scale, illustrated in Fig. (**2**) [28]. Firstly, a small amount of bacterial culture is activated on solid surfaces or in a liquid medium to obtain an inoculum to charge it into bioreactors. The production of XG and the growth of the microorganism are affected by different factors, including the bioreactor type, the operation mode, the medium constituents, and the operational conditions (temperature, dissolved oxygen concentration, and pH). Moreover, further purification includes the precipitation by miscible-water non-solvents (isopropanol, ethanol, or acetone), pH adjustments, and the addition of certain salts. The FDA regulations prescribe the use of isopropanol for the precipitation of XG. After precipitation of XG, the product is dewatered and dried, then is milled and packed into containers with low permeability to water.

2.1.4. Properties of XG

Xanthan gum includes unique features: thermal stability, non-toxicity, good compatibility, and stable through corrosive conditions [4, 48, 49]. XG color is off-white and odorless [44]. XG has an anionic character owing to the glucuronic acid groups, in addition to the pyruvate moiety over its chain [50]. XG resists the cellulases attack; however, its backbone is similar to a cellulosic structure. In comparison, its trisaccharide side chains act as a barrier to enzymatic attack. The disordered helical structure of XG only can catalyze the cleavage of the backbone when attacked with fungal cellulases, but the ordered form is not affected with fungal cellulases [25, 51]. Similar to many other gums (except starch products), XG is not digested in humans and serves to decrease the calories content of foods and improves their passage through the gastrointestinal tract (GIT). The calorific value of XG is about 0.6 kcal g^{-1} [25, 52]. In addition, XG is employed in the fabrication of suspension and emulsion as a stabilizer, thanks to 3D networks among XG chains. Also, XG is used as a thickening and suspending agent and a potent ligand for TLR4 [52-55].

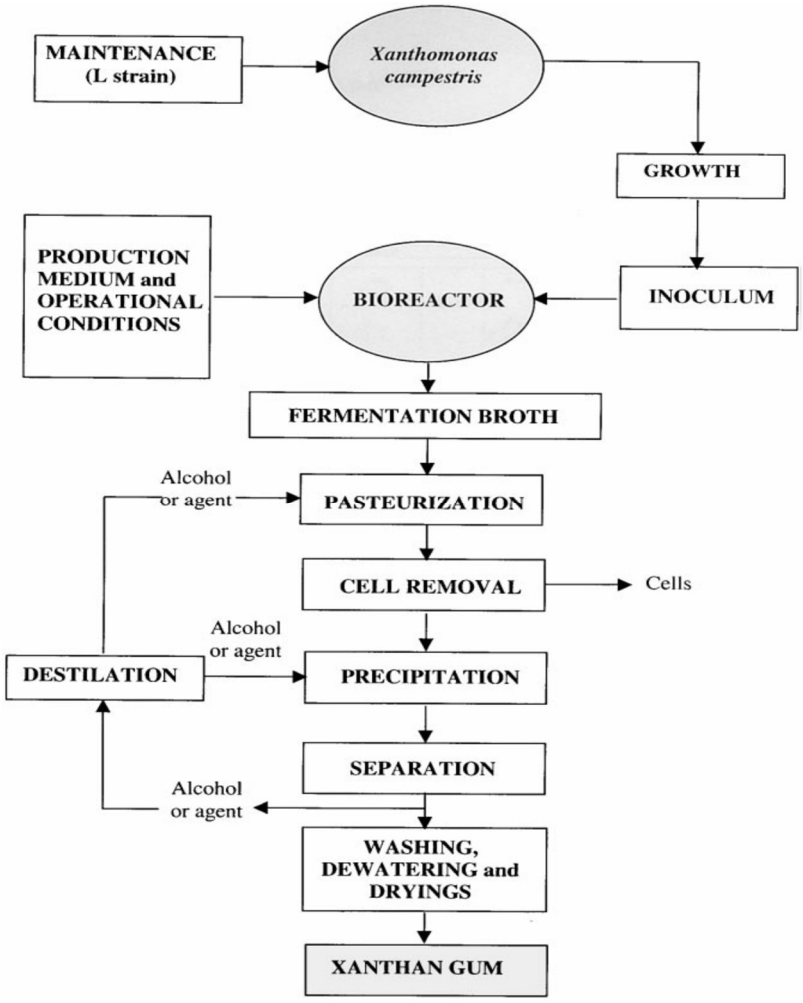

Figure 2: The production of XG using bacterial strain [28].

2.1.5. Applications of XG

XG has widely been applied in various applications: petroleum and oil industry, pharmaceutical, cosmetic, and food applications thanks to its superior pseudoplastic rheological properties [4, 28, 56].

2.1.5.1. Food Applications

XG is used in salad dressing as an emulsion stabilizer, a dispersing and a suspending agent, and a thickener. While, in soups and gravies, XG is used as a stabilizer to increase syneresis and to prevent thickness. Moreover, XG is added to bakery products to improve the cohesion of starch granules and to increase the shelf-life of products because of moisture retention. Also, it is used to control the gas entrainment and butter rheology in prepared cake mixes. While in frozen food, XG is used to improve freeze-thaw stability by binding free water. Other examples of XG in food applications are its uses as a stabilizer in desserts, topping, and dairy products [25, 28].

2.1.5.2. Cosmetic and Pharmaceutical Applications

XG is widely used in cosmetic applications, toothpaste, and personal care products. In toothpaste, XG has shear-thinning flow behavior that allows easy extrusion from the tube and keeps a stable stand on the brush. While, in personal care products such as shampoos, lotions, eye contour gels, and denture cleaners, XG is used as a thickener and as a stabilizer [25, 28, 44, 57]. Also, XG is used in pharmaceutical formulations as a thickener and as an emulsion stabilizer to prevent the separation of insoluble ingredients such as Barium Sulphate in X-ray contrast media [25, 44].

2.1.5.3. Other Applications

In the petroleum industry, XG can be used as a lubricant in drill-hole. While, in oil recovery applications, it is used in oil drilling fluids and enhanced oil recovery because XG is thermally stable under high-temperature range (up to 90^{o}C) and stable at high salt concentrations, so these superior properties of XG can reduce the water mobility by increasing the viscosity and reducing the permeability [25, 28, 44]. Furthermore, XG can be used in agricultural products as a suspension stabilizer to improve the sprayability of plants and reduce the drift and increase the cling and permanence of agricultural chemicals. Also, it can be used in jet injection printing, textile printing paste, water-based paints, toiletries, colors, adhesives, construction and building materials and texture coatings due to its rheological properties [25, 28, 33, 57, 58].

2.1.6. Limitation of XG

XG has some limitations that restrict its usage in industrial applications, including no antibacterial properties [59], poor workability and surface area [23], and slow dissolution rate [4]. These drawbacks reduce the potential uses of XG, so there are suitable chemical modifications can be done on the XG structure to overcome these drawbacks and to enable XG for use in specific drug delivery systems and wastewater treatment [23, 52, 59].

2.1.7. Modifications of Xanthan Gum

In Fig. (**1**), XG includes two highly reactive moieties that are hydroxyl (-OH) groups on each repeating unit and carboxylate (-COO^{-}) groups. They give the ability for chemical modification of XG to improve its solubility and its mechanical and physical properties.

2.1.7.1. Modification of XG with Formaldehyde

Dong *et al*. [60] improved the dissolution rate of XG through chemical modification with formaldehyde. The product was elucidated using FTIR and X-ray diffraction techniques, and their spectra showed the reduction in both intermolecular interactions and crystallinity of XG that improved the process of swelling and dissolution. The viscosity measurements showed that chemically modified XG dissolved more rapidly than native XG.

2.1.7.2. Graft Copolymerization of XG

Recently, modification of physical and chemical properties of natural polysaccharides and their derivatives through graft copolymerization technique has been attracted much attention by scientific researchers. Natural polysaccharides can be modified through graft copolymerization with various monomers onto their chains by covalent bonds to improve their characteristic properties such as water repellency, thermal stability, acid-base, and flame resistance, and dyeability. Modified natural polysaccharides are widely used in potentially new applications because they have the advantages of natural polysaccharides in addition to synthetic polymers [1, 52, 61].

There are different techniques for the synthesis of XG graft copolymers, including free radical initiators using different initiators including KPS and ceric ammonium nitrate, in addition, gamma and microwave radiations. Copolymerization graft creates different functional moieties through covalent bond onto xanthan gum structure, and it is widely used in different applications such as drug delivery and wastewater treatment [52, 62, 63]. Interestingly, the graft yield (GY) and the graft efficiency (GE) % are calculated according to the following equations (1- 2) [64-66].

$$\% GY = [(W1 - W0) / W0] \times 100 \quad (1)$$

$$\%GE = [(W1 - W0) / (W2 - W0)] \times 100 \quad (2)$$

Where W_o is the initial weight of XG while W_1 and W_2 are the weights of grafted matrix after and before purification, respectively.

2.1.7.2.1. Free Radical Graft Copolymerization of XG

Pandey *et al*. [67] reported the synthesis of grafted copolymerization of XG with poly(acrylic acid), PAA, by free radical polymerization mechanism using redox system (PMS / ferrous sulfate (Fe^{2+})) as an initiator in the presence

of sulfuric acid (H_2SO_4) (Scheme **1**). Maximum GY% was obtained as 230.4%, when [XG] was 1 gL^{-1}, [acrylic acid], [PMS], [Fe^{2+}] and [H_2SO_4] were 5.0X10^{-2}, 4.0X10^{-3}, 5.0X10^{-3} and 0.9X10^{-3} $molL^{-1}$, respectively, temperature was 35°C and time was 2h. The thermal stability of XG and its grafted copolymer (XG-g-PAA) was studied via thermogravimetric analysis, and the results illustrated thermal stability of grafted xanthan gum better than the pristine one.

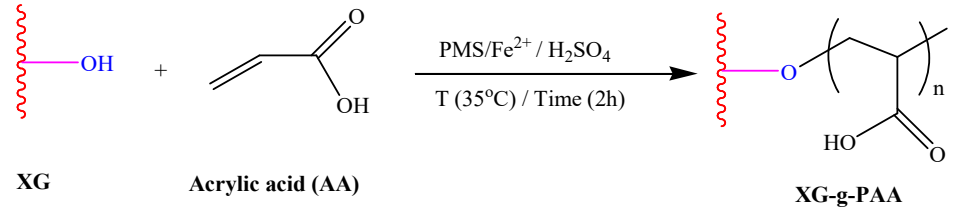

Scheme 1: Synthesis of Polyacrylic acid-grafted-XG.

Kumar *et al*. [23] improved the thermal stability of XG by graft copolymerization of poly(4-vinyl pyridine), P(4-VP) onto XG chains through free radical polymerization using PMS / ascorbic acid as a redox initiator system in an aqueous solution and in the presence of H_2SO_4 under nitrogen (Scheme **2**). The optimum grafting conditions were determined at [XG] was 0.4 gL^{-1}, [4-VP], [PMS], [ascorbic acid] and [H_2SO_4] were 0.1, 0.01, 0.01 and 0.025 $molL^{-1}$, respectively, grafting temperature was 45°C and reaction time was 2h. Thermal stability analysis showed that XG-g-P(4-VP) was more thermally stable than pure XG.

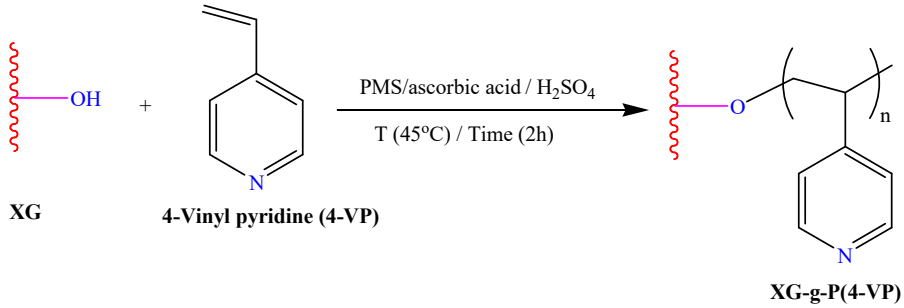

Scheme 2: Synthesis of XG-g-poly(4-vinyl pyridine) (XG-g-P(4-VP)).

Sand *et al*. [68] reported the properties of grafted xanthan gum by poly2-acrylamidoglycolic acid. Grafted XG was done by free radical polymerization technique using redox system, potassium bromate ($KBrO_3$)/thiourea, as an initiator under an inert atmosphere (Scheme **3**). The optimum grafting conditions were determined at [XG] =1.0 gL^{-1}, [2-Acrylamidoglycolic acid] = 5.3X10^{-2} $molL^{-1}$, [BrO_3^-] = 10X10^{-3} $molL^{-1}$, [thiourea] = 2.8X10^{-3} $molL^{-1}$, [H_2SO_4] = 4.0X10^{-3} $molL^{-1}$, reaction temperature was 40°C and reaction time was 2h. Thermal stability results illustrated thermal stability of grafted xanthan gum better than the pristine one. Also, water swelling capacity studies were done on grafted copolymers, and the results proved that the swelling ratio increased with increasing the grafting ratio. Moreover, XG-g-poly (2-Acrylamidoglycolic acid) was resistant to biodegradation and was able to remove toxic heavy metal ions such as nickel ions (Ni^{2+}), lead ions (Pb^{2+}), and zinc ions (Zn^{2+}) from its aqueous solutions.

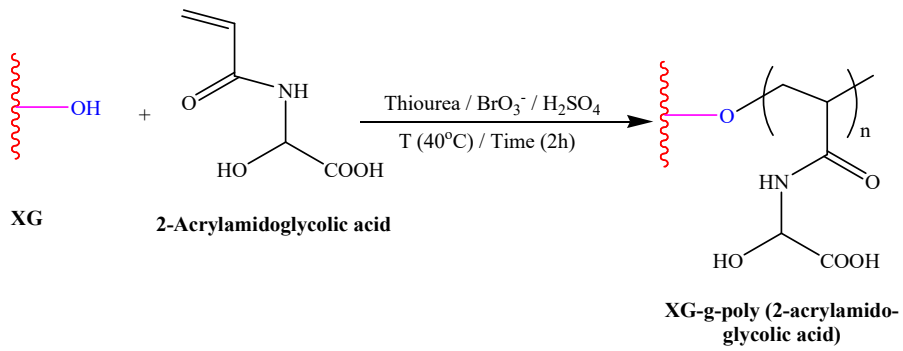

Scheme 3: Synthesis of XG-g-poly(2-Acrylamidoglycolic acid).

Pandey and Mishra [69] prepared free radical grafted XG by poly (ethyl acrylate), XG-grafted-PEA using potassium persulfate (Scheme **4**). The GY% and GE% decreased with increasing XG, and they increased with decreasing ethyl acrylate and PPS concentrations. optimum conditions were [XG] = 4.0 gL^{-1}, [ethylacrylate] = $17.0X10^{-2}$ $molL^{-1}$, [PPS] = $35.0X10^{-3}$ $molL^{-1}$, grafting temperature was 45°C and grafting time was 1h. Thermal analysis data revealed that XG-g-PEA was more thermally stable than native XG. The adsorption ability of grafted XG was studied against the adsorption of Zn^{2+} ions, and the results showed that grafted copolymer was used as an efficient remover of Zn^{2+}ions from its aqueous solution.

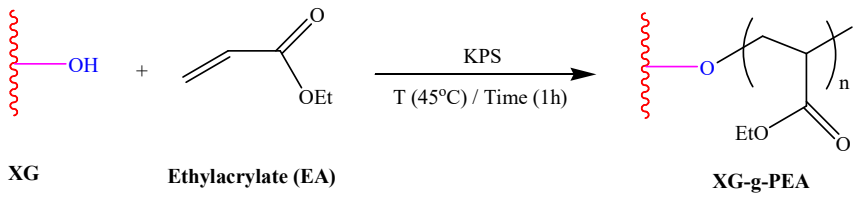

Scheme 4: Preparation of grafted XG by poly(ethyl acrylate).

Mundargi *et al*. [70] synthesized XG-g-poly(acrylamide),(PAAM), by free radical initiation polymerization of acrylamide monomer onto XG chains using two different ratios of XG to acrylamide (1:5 and 1:10) with CAN as an initiator under nitrogen atmosphere (Scheme **5**). XG-g-PAAM was used as a carrier for antihypertensive drugs such as atenolol (ATL). The *in vitro* drug release time continued up to 24h for releasing 85% from drug-loaded in simulated gastric fluid (SGF) followed by simulated intestinal fluid (SIF) media. Also, the released time increased with increasing the grafting yield of grafted XG.

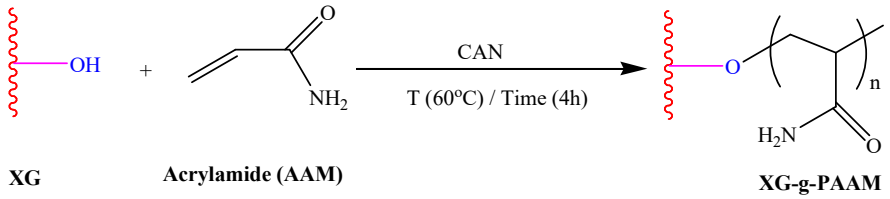

Scheme 5: Synthesis of XG-g-poly(acrylamide).

2.1.7.3. XG Hydrogels

2.1.7.3.1. Hydrogels

Hydrogels are hydrophilic three-dimensional polymeric networks that are prepared chemically or physically by the cross-linking method using natural and synthetic polymers [71]. They have different hydrophilic functional moieties, including carboxylic and hydroxyl, as well as sulphonyl, imide, and amide groups on polymer chains. So, they can capture both water and biological fluids through their structure compositions. Also, hydrogels are known as hydrophilic gels and aqua gels [72-75]. In addition, their swelling ability can be controlled by various parameters such as the presence of hydrophilic functional groups, the nature of the cross-linking agent, and the polymerization technique.

The nature of cross-linking agents for the formation of 3D polymeric networks is divided into physical and chemically cross-linking agents. In chemically cross-linked hydrogels that are also known as either thermosetting hydrogels or permanent gels, the polymer chains are covalently bonded using a chemical cross-linking agent. While, in physically cross-linked hydrogels, the polymers are connected via H-bonding or electrostatic interactions. The responsiveness of polymeric hydrogels is enhanced with different external factors such as pH, electric field, light, temperature, or ionic strength [74, 76-80].

Moreover, hydrogels demonstrate dual nature with different properties on both macroscopic and microscopic scales. They are found as a solid with a definite shape on the macroscopic scale. In contrast, on the microscopic scale, their behavior is similar to solutions. In addition, hydrogels can be used as a molecular filter in biological sciences because they can trap water-soluble molecules. So, they are essential in electrophoresis [74, 81]. Hydrogels include different groups based on their physical behavior, electric charges, sources (origin), and nature

of cross-linking agents (Fig. **3**) [74]. Hydrogels have been widely used in various fields such as tissue engineering as scaffolds and cell culture, drug delivery, wastewater treatment, and antimicrobial fields [82-88].

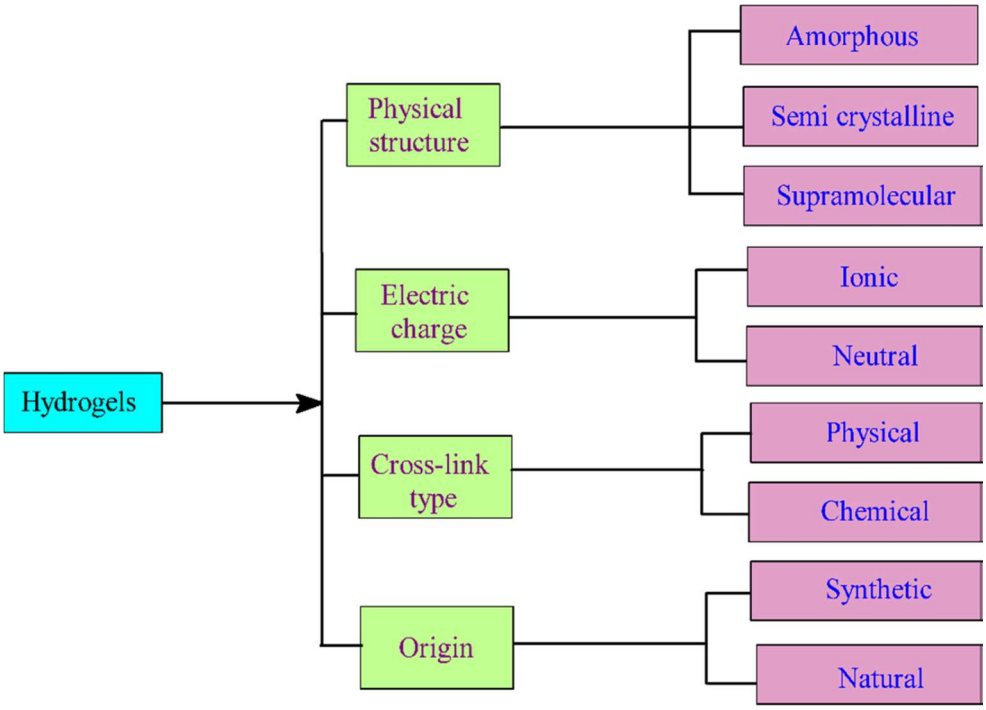

Figure 3: Classification of hydrogels according to different categories [74].

Bejenariu *et al.* [49] reported XG/ sodium trimetaphosphate, STMP chemically hydrogels (Scheme **6**). XG / STMP hydrogels were synthesized in the presence of different STMP: XG ratios. The hydrogels showed inverse proportional of the swelling ability with hydrogel concentration, in addition to phosphate charges. Increasing the amount of cross-linking agent led to a decrease in the swelling rate due to stiffening the hydrogel networks and generating the anionic phosphate charges that electrostatic repulled with neighboring XG chains; thus, it had a positive effect on swelling behavior. Maximum swelling capacity reached 120 gg^{-1} at STMP:XG ratio (10:1). In addition, XG / STMP hydrogels were pH sensitive, so the maximum value of the swelling behavior was observed at pH7 compared to the acidic and alkaline media. At alkaline medium (pH 13), the swelling rate decreased due to the collapse of the hydrogel networks caused by the Na^+ cationic counterions charge screening effect that shielded the anionic electrostatic repulsion of the phosphate anionic charges. While, at acidic medium (pH 3), the hydrogen ions interacted with phosphate anions which diminished the electrostatic repulsive forces that led to a decrease of the swelling rate. However, at a neutral pH medium, the phosphate groups became ionized, and electrostatic repulsions caused the increase in swelling rate.

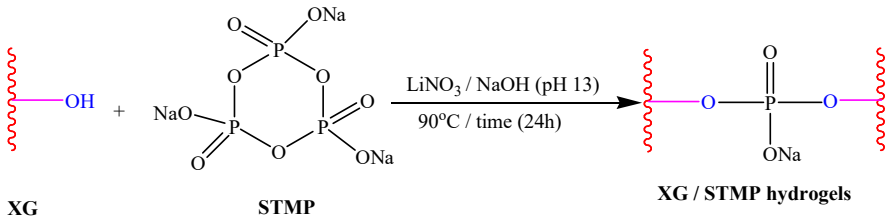

Scheme 6: Synthesis of XG / STMP hydrogels.

Gils *et al.* [89] reported that chemically cross-linked super porous XG hydrogels were synthesized using two monomers: HEMA (2-hydroxyethyl methacrylate) and AA (acrylic acid) using APS and TMED and methylene bisacrylamide, sodium bicarbonate ($NaHCO_3$) and triblock copolymer (Lutrol F® 127) as a cross-linking agent,

foaming agent and foam stabilizer, respectively (Scheme **7**). The hydrogels were investigated using different tools, including Fourier Transform Infrared (FTIR), thermogravimetric analysis (TGA), scanning electron microscopy (SEM), high-performance liquid chromatography (HPLC), and gas chromatography (GC). The swelling ability of XG-g-poly (AA-co-HEMA) hydrogels was studied in different swelling media (different environmental pHs and salt solutions. At acidic pH values (1-3), the hydrogen ions protonated most of $-COO^-$ anions; thus, the swelling ability of hydrogels declined. While, at higher pH values (5-7.4), the swelling capacity of hydrogels increased due to the ionization of some $-COO^-$ anions that led to an increase in the electrostatic repulsive forces between carboxylate anions. However, at alkaline pH (pH > 7.4) medium, Na^+ counterions had a charge screening effect that decreased the swelling behavior of XG hydrogels. While, the results of swelling behavior of XG hydrogels in various salt solutions (NaCl, $CaCl_2$, and $AlCl_3$) demonstrated that noticeably decreased swelling ability of hydrogels in salt solutions compared with their swelling in distilled water due to the charge screening effect of added cations that led to diminishing the anion-anion repulsive forces. Moreover, a biodegradation study of tested samples was tested in *Streptococcus bovis* (*S. bovis*) medium, and the results exhibited that homopolymer (poly (acrylic acid)) had the best biodegradation rate by weight loss in *S. bovis* medium. At the same time, the synthesized XG-g-poly (AA-co-HEMA) hydrogels showed a higher biodegradation rate than in the case of copolymer (poly (AA-co-HEMA)) and PHEMA homopolymer.

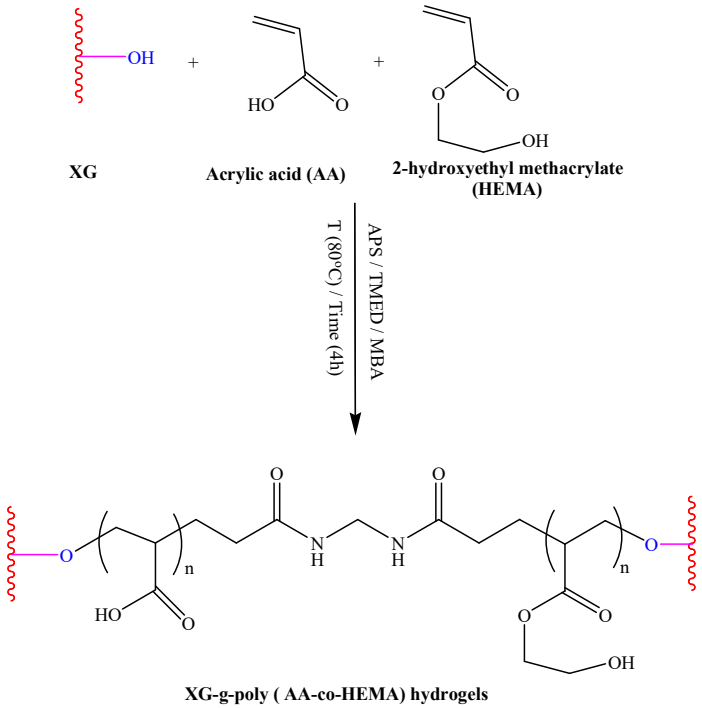

Scheme 7: Synthesis of XG-g-poly (AA-co-HEMA) hydrogels.

Shalviri *et al.* [90] synthesized chemical cross-linked starch / XG hydrogels in the presence of different concentrations of STMP (cross-linking agent) and XG for controlled drug delivery (Scheme **8**). XG hydrogels were elucidated via solid ^{31}P NMR spectroscopy, SEM, and FTIR. The swelling behavior of hydrogels was studied in different pH values (from 2 to 12), and the results demonstrated that the swelling rate of cross-linked hydrogels increased with increasing both XG and STMP concentrations. Also, the gel mesh sizes of hydrogel films were investigated, and the results showed that hydrogels mesh size increased with an increase in swelling ratio, and it varied from 2.84 to 6.74 nm depending on the hydrogel compositions. Moreover, the permeability of different drugs such as ibuprofen sodium salt, sodium salicylate, caffeine, methylene blue, vitamin B12, pyrogallol red, and fluorescein isothiocyanate-dextrans with varying content of XG and STMP was measured using side-by-side diffusion cells. The results exhibited that the selective permeability of cross-linked hydrogels depended on drug charges, so the permeability of anionic drugs through starch / XG films was less than their neutral form because of the electrostatic repulsive forces between anionic drugs and starch / XG hydrogels.

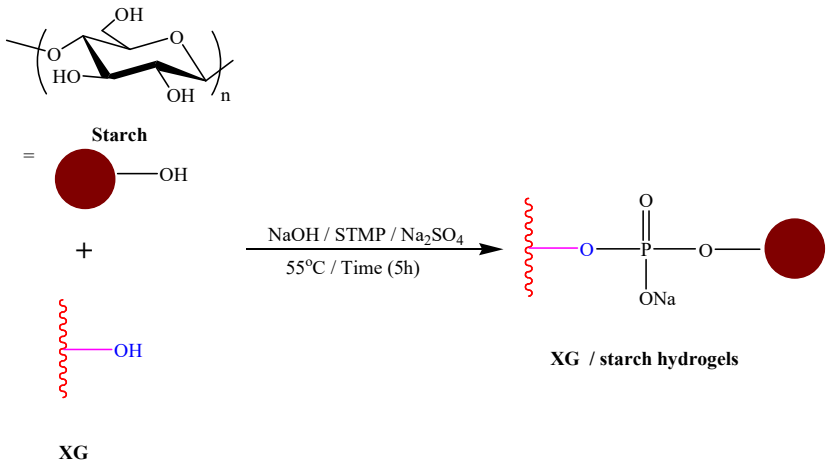

Scheme 8: Synthesis of cross-linked XG / starch hydrogels.

Argin *et al.* [91] synthesized polyelectrolyte complex (PEC) hydrogels based on XG as an anionic polysaccharide and chitosan (Ch) as a cationic polymer through electrostatic interactions (Scheme **9**). Probiotic bacteria (*Pediococcus* (*P.*) *acidilactici*) cells were mixed with XG, and Ch solutions were frozen dry in the form of capsules. Moreover, the bacterial cells released from XG /Ch PEC capsules were investigated in deionized water, SGF (pH 2), and SIF (pH 6.8). The findings showed the negligible release of *P.acidilactici* cells in deionized water for 72h due to the stability of XG / Ch capsules in deionized water. Also, it demonstrated that the cell released from XG / Ch PEC capsules in SGF at pH 2 after 2 hr exposure is negligible. In contrast, the cell released from PEC capsules was completed in SIF after 5 hr. The previous results suggested using XG / Ch PEC capsules as good delivery material for the probiotics to the intestines.

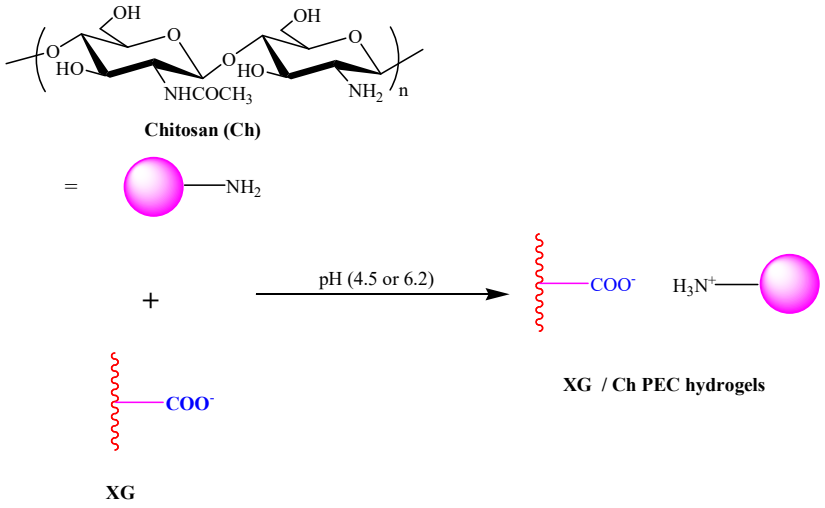

Scheme 9: Synthesis of XG / Ch PEC hydrogels.

4. Applications of Xanthan Gum

4.1. Protein Delivery System

4.1.1. Bovine Serum Albumin

Bovine serum albumin (BSA) is a natural protein with an isoelectric point (pI) of 4.8. Therefore, BSA includes negative charges at pH 7.4 (physiological pH). Moreover, BSA is vastly applied in many fields like biomedical and pharmaceutical, in addition to drug delivery due to its fabulous features such as biocompatible, biodegradable, safe material, no immunogenicity, excellent stability, and low-cost material. In addition, BSA is used as a shielding agent to prevent non-specific adsorption, and it is widely used in diagnosis tests [92-96].

Bueno and Petri[95] prepared two different XG hydrogel films by casting technique in the absence and presence of citric acid, XGH, and XCA, respectively, at 45°C overnight. Citric acid is a biocompatible and non-toxic cross-linking agent. Moreover, the ability of XGH and XCA films to load and release two globular proteins, BSA and lysozyme (LYZ), was controlled by proteins net charges and hydrogels. For BSA, XGH films are more appropriate than XCA films because of their low charge density that avoids the electrostatic repulsive forces. Moreover, BSA was completely released from XGH films after 1 hr through pH values from 2 to 10. In comparison, the loading and release of LYZ showed that XGH and XCA films are efficient carriers for LYZ. At pH 7.0, the release of LYZ was very low because of the electrostatic forces between LYZ and hydrogels.

Maiti *et al.* [97] synthesized BSA-loaded carboxymethyl xanthan gum microparticles by modifying XG to carboxymethyl xanthan gum (CMXG) in the presence of sodium hydroxide and mono-chloroacetic acid and then cross-linked through its carboxylate groups with aluminum chloride ($AlCl_3$) as cross-linking agent. BSA encapsulation efficiency (EE) of microparticles was studied in the presence of different BSA concentrations (30, 40, and 50% (w/w)), and the pH of CMXG solution was adjusted to 6 and 7. The results illustrated that increasing the concentration of BSA added led to a decrease in the EE % of CMXG microparticles due to the diffusion of BSA into the aqueous gelation medium. So, at pH 6 of CMXG solution, EE % was found 82.27 % to 72.04 % when the BSA concentration was added from 30% to 50% (w/w), respectively. While at pH 7, EE % was obtained 81.22 % to 68.75 % at the same BSA concentrations. Moreover, *in-vitro* release of BSA from BSA-loaded microparticles was investigated in pH 1.2 through 2h and pH 7.4, and the results presented a faster release of BSA in acidic buffer more than BSA released in PBS medium. It was accounted for the highest swelling ability of CMXG microparticles in an acidic medium.

Magdy *et al*.[98] reported the encapsulation of BSA with biocompatible XG / poly (*N*-vinyl imidazole (PVI) hydrogels (Fig. **4**). The results showed that % BSA loading (DL%) and % encapsulation efficiency (% EE) increased with the increase in both gelation time and loaded BSA concentration, whereas they decreased with an increase of the polymer concentration. So, the maximum value of %DL and %EE was 59.50% and 99.17%, respectively. In this study, the in-vitro BSA release was studied in PBS (pH 7.4), and the findings exhibited the increase of hydrogel concentration led to an increase in BSA release. Moreover, the kinetic studies of the BSA release from hydrogel matrix followed non-Fickian and case II transport mechanisms.

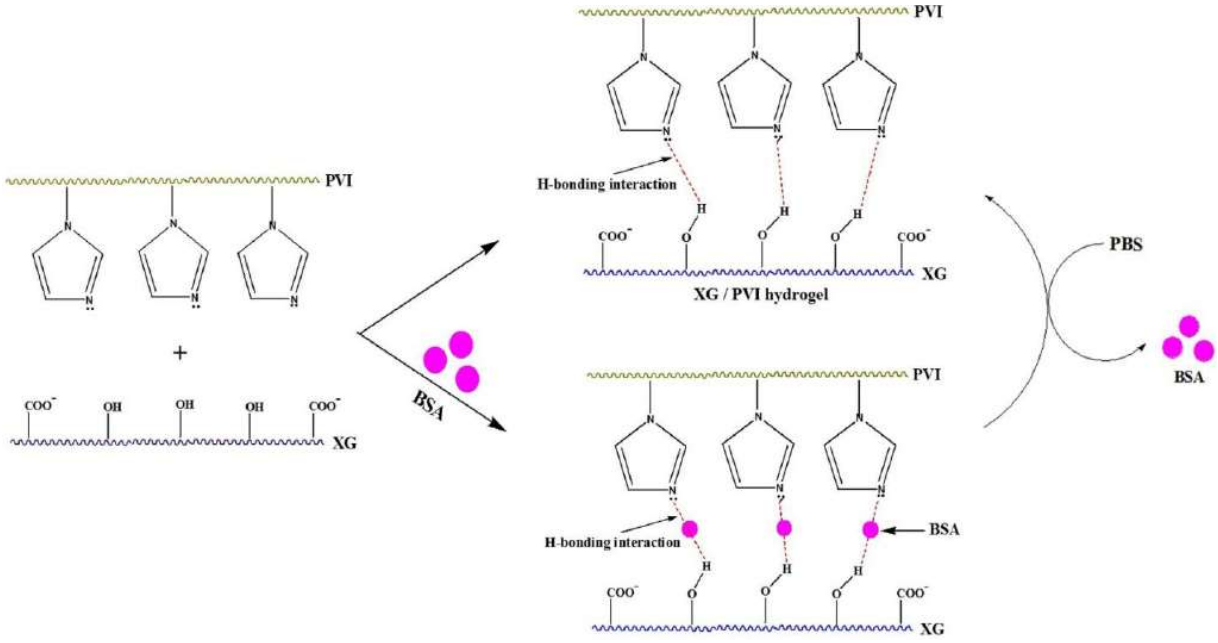

Figure 4: Schematic preparation of encapsulation of BSA with biocompatible XG / poly (*N*-vinyl imidazole (PVI) hydrogels [98].

Mohamed *et al*. [24] demonstrated the preparation of antimicrobial pH-sensitive drug carriers to encapsulate BSA as a protein drug model using cross-linked XG-g-PVI hydrogels and MBA as a crosslinker for delivery of protein

in the intestines. BSA loading and release from loaded hydrogels were tested in two pHs media, such as pH 1.2 and slightly alkaline (pH7.4) solution, mimicking simulated gastric and intestinal media, respectively, through different time intervals at 37°C. The results exhibited an increase in both swelling rate and accumulative BSA release in pH 7.4 than acidic pH. Additionally, the BSA release mechanism followed the non-Fickian release mechanism. Cytotoxicity of hydrogels was investigated against normal cell line by a neutral red uptake assay test, and the results illustrated that the prepared hydrogel-based BSA carriers possess good biocompatibility and are considered a safe carrier for protein delivery. Moreover, the authors investigated the antimicrobial property of the as-prepared hydrogels against Aspergillus niger and Staphylococcus aureus, and the reported findings confirmed the examined hydrogels could be used as antimicrobial protein carriers to deliver the proteins through the gastrointestinal tract.

Recently, in this approach, Abu Elella *et al*. [99] reported the fabrication of biodegradable interpolyelectrolyte complex hydrogel as a pH-sensitive protein carrier. They prepared interpolyelectrolyte complex based on XG and trimethyl-N-quaternized chitosan (TMC) to solve the drawbacks of the protein delivery through the GI tract. The BSA loading and release were examined in gastric simulated pH (pH 1.2) and intestine simulated pH (pH 7.4). The maximum DL% and EE% were 52.0% and 91.7%, respectively. On the other hand, the BSA release results showed that the amount of BSA released in pH 7.4 was higher than in pH 1.2 and also went up with the rise within the amount from 12 to 120 hr to be 97.9% in pH 7.4 and 29.7% in pH 1.2 at 120 h.

Table 1: Different hydrogels composition based on modified xanthan gum for protein delivery.

Hydrogel Composition	Protein Type	Protein Loading % (DL%)	Encapsulation Efficiency (EE%)	References
Xanthan gum / citric acid	BSA Lysozyme	30.0 24.0	15.0 10.0	[95]
Carboxymethyl xanthan gum / $AlCl_3$	BSA	-	82.27	[97]
XG / PVI	BSA	59.50	99.17	[98]
XG-g-PVI / MBA	BSA	49.20	99.90	[24]
XG / TMC	BSA	52.0	91.70	[99]

- Means not reported.

4.2. Wastewater Treatment

Drinking water is an essential source for all individuals' lives worldwide. Therefore, water contamination is a lethal environmental problem worldwide. In addition, it has attracted global concern because of the rapid growth rate of industrialization [100-102]. In recent years, water has been polluted with different synthetic dyes and their intermediates products [103, 104]. Synthetic dyes are applied in different industries, for instance, textile, ink, paper, etc., owing to their easy availability and low price [105]. In addition, the statistical studies showed that 10% of used dyes are discharged into industrial effluents in different water sources due to their lower efficiency in the dyeing process [106].

Furthermore, dyes are dangerous compounds since they are toxic, highly carcinogenic, and non-biodegradable. So, they accumulate inside human body cells and cause fatal effects on human health [105, 107]. Elimination of dyes is a complicated process because of their complex aromatic structure and synthetic origin, which make them stable against biological degradation [107-110]. Among them, crystal violet (CV) dye is widely used for dyeing leather, nylon, paper, cotton, wool, and silk. Also, it is used as a bacteriostatic agent in aquaculture [111-113]. Moreover, CV can be detected from both aquaculture water samples and processed fish products[114, 115]. For example, Abu Elella *et al*. [116] reported the facile and green method to prepare dual-functional adsorbent hydrogel for capturing crystal violet dye and toxic microorganisms such as *Escherichia coli* (Fig. 5). They prepared interpenetrating networks hydrogel based on XG and TMC. The adsorption capacity results showed that maximum adsorption capacity was reported of 94.4% and Qmax of 555.6 mg/g.

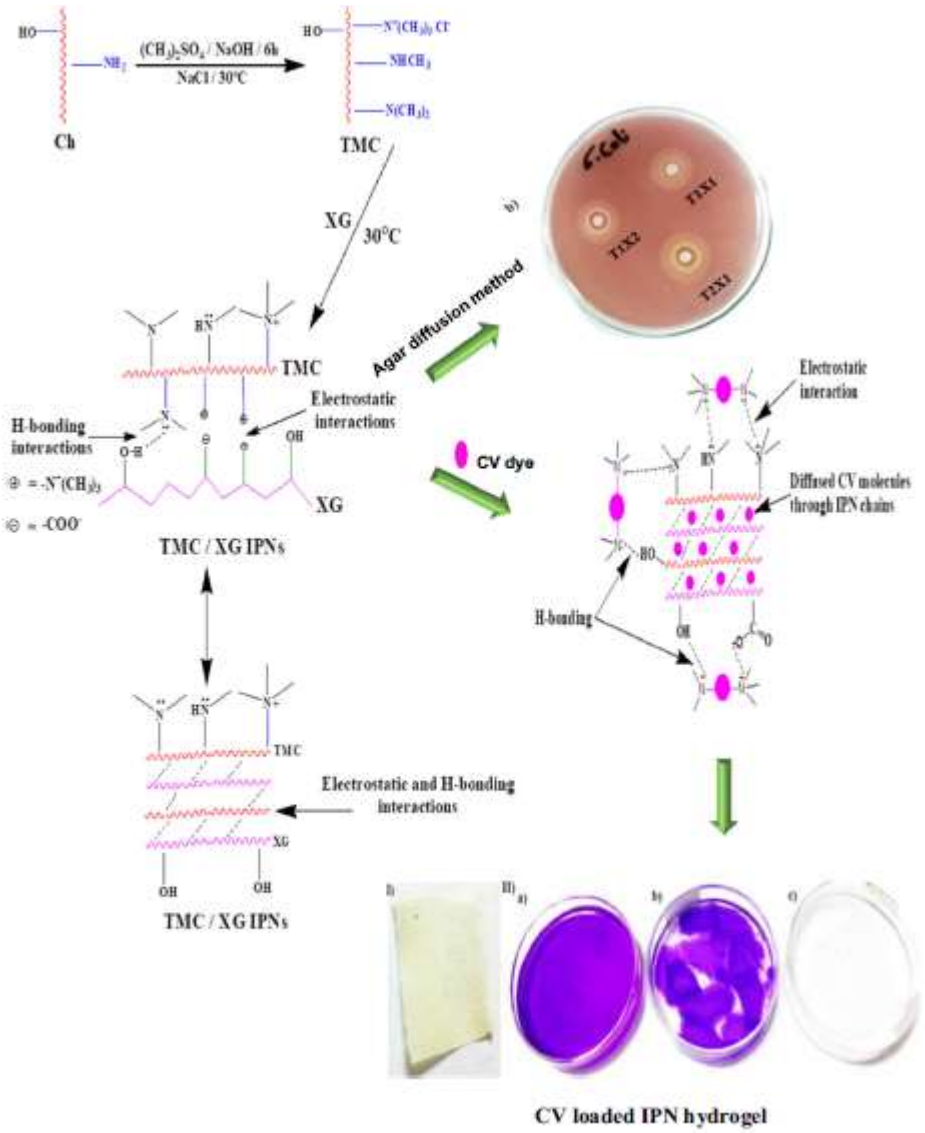

Figure 5: Schematic preparation and adsorption of crystal violet using XG / TMC hydrogels.

On the other hand, malachite green (MG) dye is another toxic cationic synthetic dye with the molecular formula C_{23} H_{25} Cl N_2. Furthermore, the toxicity of MG dye owing to its hazardous effects on the ecosystem, following various diseases. MG color remains for a long time in water and does not readily degrade [117-120]. Recently, Abu Elella *et al*. [37] reported the fabrication of antibacterial nanocomposite adsorbent based on biodegradable polymers for removal of both MG and pathogenic microorganisms as E.coli and S. aureus as the most common pollutants for water. They prepared XG-grafted-PVI nanocomposites in the presence of biocompatible nanofillers as Montmorillonite clays. The adsorption findings showed maximum adsorption was reported of 909.1 $mg.g^{-1}$ through different interaction bonds such as electrostatic bonding interaction, as well as hydrophobic interaction (Fig. **6**). Also, the adsorption results well fitted the Langmuir isotherm model, and the antibacterial assay results exhibited excellent inhibition growth of nanocomposites against two examined bacteria.

To extend its potential uses, XG has been chemically modified to form a hydrogel and nanocomposites-based XG, which is used as an adsorbent in wastewater treatment [105, 107, 121-125]. Incorporation of Fe_3O_4 MNPs into XG-g-PAA to form nanocomposite hydrogel was found effective in capturing of MV dye from contaminated water with an efficiency of 99%, and Q_{max} of 642 mg/g at a contact time of 60 min, optimum pH of 6.5 at 25 °C [107]. Additionally, modified XG with poly (acrylic acid) and graphene oxide nanocomposite was tested as adsorbent for MB dye. The as-prepared nanocomposites exhibited good stability and excellent adsorption for MB dye with an increase in GO contents up to 88.5% of MB dye, fitting the second-order kinetic model [126].

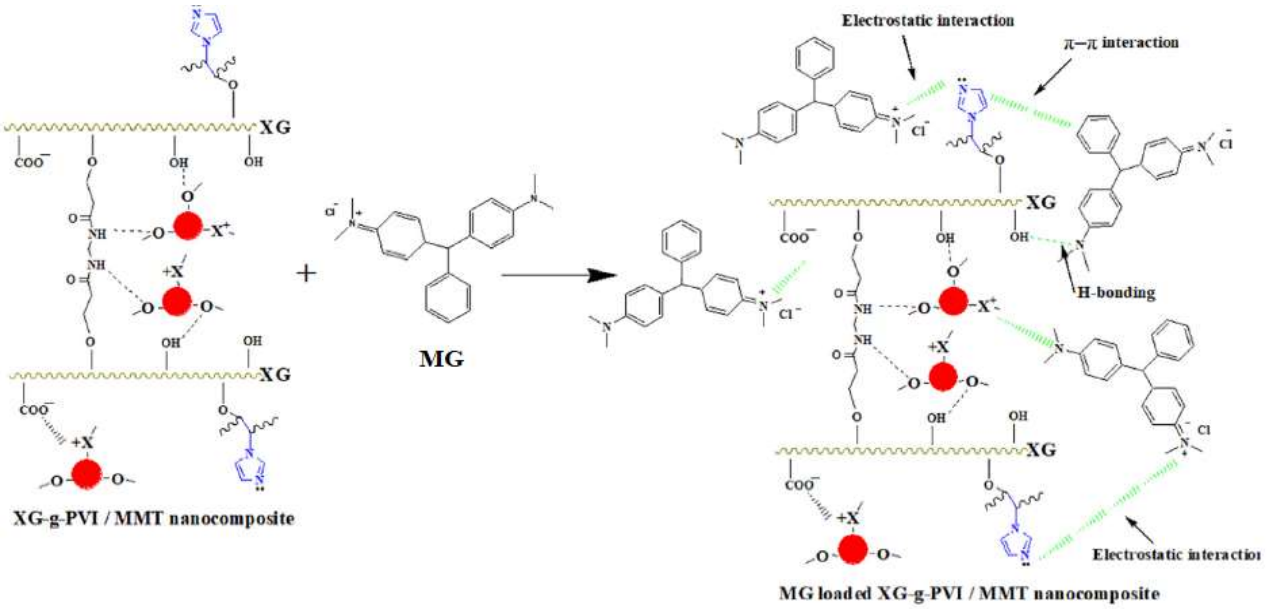

Figure 6: The schematic diagram for removal of MG using XG-g-PVI/MMT nanocomposite.

In another interesting study, Ghorai *et al*. [121] utilized bio-degradable h-XG/SiO_2 nanocomposites adsorbent via the sol-gel process to capture MV and MB dyes, which is presented in Fig. (**7**). Maximum adsorption of dyes was mentioned of 99.4% for MB and 99.1% for MV dyes. The Q_{max} 497.5 mg/g for MB dye at pH 8 at a contact time

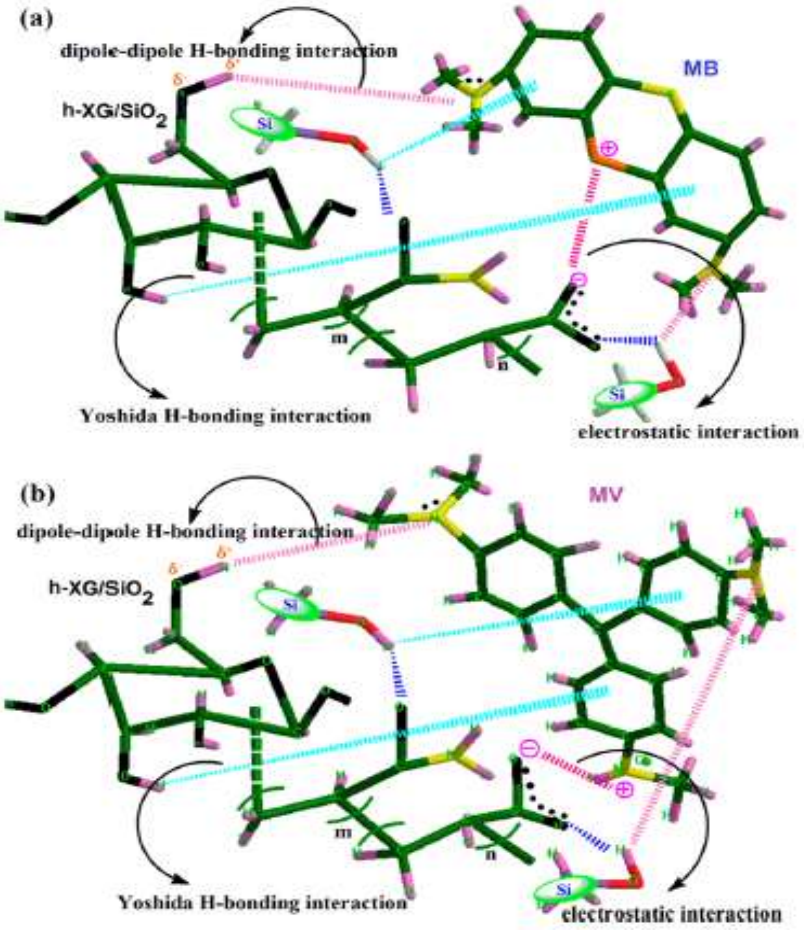

Figure 7: Schematic layout of h-XG/SiO2 nanocomposite adsorbent for removal of MV and MB dyes [121].

of 20 min, and temperature of 323 K. Meanwhile, Q_{max} for MV was 378.8 mg/g at pH 9 at a contact time of 15 min, and temperature of 313 K. Also, Ghorai *et al*. [122] demonstrated the preparation of XG-g-PAM/SiO_2 nanocomposites for the removal of Congo red as a toxic dye. Preparation of the as-prepared nanocomposite was done by *in situ* inclusion of Si NPs onto its surface, fabricating with a sol−gel approach. The excellent adsorption capacity was recorded of 209.2 $mg.g^{-1}$. Another interesting study was performed for the effective removal (85%) of the same dye from aqueous solutions by a novel yet green nanocomposite of xanthan gum/Methionine-bentonite (XG/Meth-bent) [127]. XG/Meth-bent nanocomposite was efficiently synthesized and confirmed by characterization analysis using several techniques such as FTIR, SEM, XRD, TGA, and zeta potential analysis. The surface area was 71 mg^2g^{-1}, and the adsorption findings showed a strong dependence of the dye removal on the pH and temperature of the solution and contact time. Moreover, Chen *et al*. [128] also reported the preparation of HA nanocomposite based on maleic anhydride-modified XG for capturing MB dye with a relatively high value of Q_{max} (769 mg/g).

Additionally, an effective eco-friendly adsorbent for dye uptake based on green modified XG hydrogels was prepared according to Chaudhary *et al*. [129]. They grafted copolymer of acrylic acid-co-itaconic acid (PAA-co-PIA) on XG/psyllium hybrid backbone under the microwave irradiation in the presence of glutaraldehyde as a cross-linking agent to be used as a good adsorbent for wastewater treatment for the removal of auramine-O, Aur-O (cationic dye) and eriochrome black-T, EBT (anionic dye). They obtained high adsorption efficiency as 95.63% and 90.53% for Aur-O and EBT dyes, respectively. Different XG formulations for the removal of various toxic dyes are reported in Table **2**.

Table 2: Different Xanthan gum formulations for removal of various toxic dyes.

Xanthan Gum Formulations	Toxic Dyes	Q_{max}(mg g^{-1})	References
XG/acrylic acid/acrylamide superporous hydrogel	Methyl violet	287.54	[130]
XG/polyacrylic acid/Fe_3O_4nanocomposite hydrogel	Methyl violet	642.0	[107]
XG/Si NPs nanocomposite	Methylene blue Methyl violet	497.50 378.80	[121]
XG/SiO_2 NPs nanocomposite	Bismarck brown Y Methylene blue	448.43 432.90	[124]
XG/Meth-bentnanocomposite	Congo red	530.55	[127]
XG-g-PAM/SiO_2 nanocomposite	Congo red	209.21	[122]
XG/Fe_3O_4 nanocomposites hydrogel	Malachite green	497.15	[105]
XG-g-PVI/MMT nanocomposite	Malachite green	909.10	[37]
XG-g-PVI/SiO_2 NPs nanocomposite	Malachite green	588.20	[131]
XG/PVI hydrogel	Crystal violet	453.0	[132]
XG-g-PVI/MBA hydrogel	Crystal violet	625.0	[133]
XG/TMC hydrogel	Crystal violet	555.6	[116]
XGTTE hydrogel	Crystal violet	35.12	[134]

As noted earlier, the nanocomposite-based adsorbents have been synthesized via infusing or incorporation of the inorganic nanoparticles onto the polymers such as xanthan gum, alginate, chitosan, cellulose, ion-exchangers, and porous resins to develop hybrid adsorbents, which can facilitate the rapid removal of metals from contaminated water [135-137]. In this view, XG-g-polyacrylamide (PAM)/SiO_2 was fabricated as a novel hybrid bio-adsorbent to eliminate Pb^{2+} from contaminated water efficiently [137]. XG-g-PAM was prepared through a radical polymerization method using potassium persulphate (KPS) as the initiator. In situ dehydration and sol-gel processes were utilized for the synthesis of the hybrid nanocomposite. The nanocomposite adsorbent exhibited excellent adsorption capacity (Q_{max} = 537.634 mg/g) of Pb^{2+} (400 ppm) at pH 5.5 in comparison to XG-g-PAM and XG. This was attributed to the enhanced hydrodynamic radius and high intrinsic viscosity of the nanocomposite

due to the uniform distribution of SiO_2 in XG-g-PAM polymer. Figs. (**8a, b**) show the adsorption mechanism of Pb^{2+} by grafted polymer and the nanocomposite and the influence of contact time on the adsorption efficiency using nanocomposite, different graft copolymers, and XG adsorbents. Additionally, Lai *et al*. [138] integrated the hierarchical GO/XG/TiO_2 nanocomposite with high thermal stability and porous sponge structure as an adsorbent for Pb^{2+} ions with maximum adsorption of 199.22 mg/g at 70°C through a costive and ice-templating method.

Ahmad *et al*. [139] illustrated the preparation of XG/n-acetyl cysteine-Mica (XG/NAC-MC) hydrogel nanocomposite for capturing different toxic heavy metals, including Pb^{2+}, Cu^{2+} and Ni^{2+} ions from aqueous solution. Structural characterization of the bionanocomposite was performed by EDX, SEM, FTIR, XRD, and TGA-DTG analysis. The adsorption of examined metal ions was significantly increased owing to different functional groups on XG/NAC-MC. The maximum adsorption of Pb^{2+}, Cu^{2+}, and Ni^{2+} ions was at pH4 and pH5 through adsorption times of 60 min and 120 min. The maximum adsorption of Pb^{2+}, Cu^{2+} and Ni^{2+} were 99.0%, 97.0%, and 93.0%, with Qmax of 530.5, 177.2 and 51.5 mg g^{-1}, respectively.

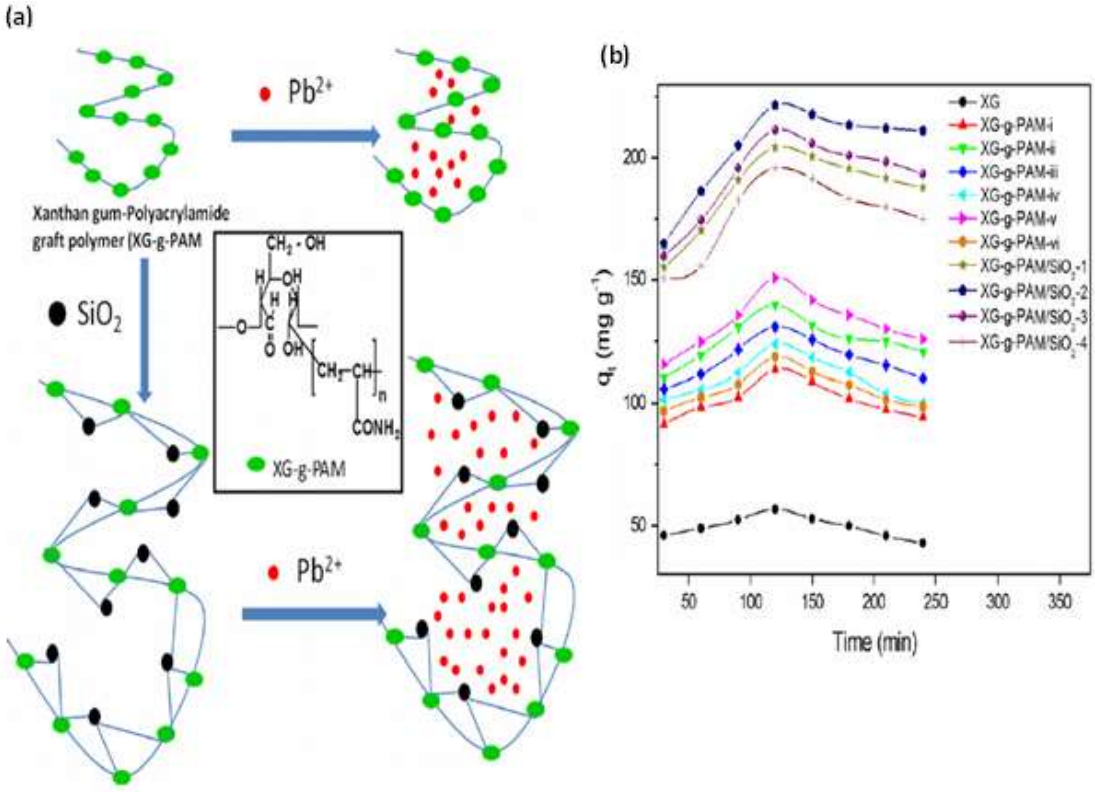

Figure 8: (a) Schematic illustration of the adsorption mechanism of Pb^{2+} by grafted polymer and the nanocomposite, (b) influence of contact time on the efficiency of Pb^{2+} adsorption using nanocomposite, different graft copolymers, and XG adsorbents [137].

In another approach, MMT nanoclays have been used as biocompatible filler to fabricate XG-grafted-poly (2-acrylamido-2-methyl-1-propane sulfonic acid, AMPS) by Jalali *et al*. [140] using APS as initiator and MBA as a crosslinker for capturing of Cu^{2+} ions. Jalali *et al*. employed the synthesized XG nanocomposite to capture Cu^{2+} ions with Q_{max} of around 29.50 mgg^{-1} at reported optimum conditions of [Cu^{2+}] = 321.80 ppm, the temperature 45.0°C, pH 5.20, and adsorption time 5 hr.

Zheng *et al.* [134] mentioned the preparation of grafted PAM/XG hydrogel using PPS and TTE (trimethylolpropane triglycidyl ether) as a cross-linking agent with various weight ratios from 2% to 6 % (w/w). The as-prepared hydrogel was investigated using different analysis tools, including FTIR spectroscopy, X-ray diffractogram, SEM, and differential scanning calorimetry (DSC). FTIR results showed the characteristic peaks at 3449, 1655, 1611, and 1420 cm^{-1} that confirmed the modification of XG. In addition, the data of XRD illustrated the increase of TTE concentration led to an increase in the intensity of the diffraction peak of XG hydrogels to reach a

maximum at 4 % (w/w) of TTE dosage. It referred to strong intramolecular and intermolecular H-bonding in XGTTE hydrogels that improved the molecular arrangement regularity. The thermal analysis results through the DSC thermogram exhibited that modified XG with AM and TTE led to an improvement in XG's thermal stability. After that, the SEM surface morphology results indicated that grafted XG with more porous honeycomb-like structure. Moreover, XG hydrogels were used to adsorb CV from an aqueous solution using 50 mg of XGTTE in 100 mL of 30 mgL^{-1} of CV for 24h at 25°C. The obtained data revealed that the maximum adsorption capacity of XGTTE2, XGTTE3, XGTTE4, XGTTE5, and XGTTE6 was 28.13, 33.09, 35.12, 34.03 and 30.39 mgg^{-1}, respectively. Different XG formulations for removing various toxic metal ions from an aqueous solution are reported in Table **3**.

Table 3: Different Xanthan gum formulations for the removal of various metal ions from aqueous solution.

Xanthan Gum Formulations	Toxic Metal Ions	Q_{max}(mg g^{-1})	References
XG/NAC-MC nanocomposite	Pb^{2+} Cu^{2+} Ni^{2+}	530.54 177.20 51.48	[139]
XG/Silica/calcium alginate	Pb^{2+}	18.9	[141]
XG-g-polyacrylamide/SiO_2 nanocomposite	Pb^{2+}	537.63	[137]
GO/XG/TiO_2 nanocomposite	Pb^{2+}	199.22	[138]
Metal ion imprinted XG/inorganic matrix	Sc Nd Tm Yb	132.30 14.01 18.15 25.73	[142]
XG-grafted AMPS hydrogel	Cu^{2+}	29.5	[140]

4.3. Antibacterial Hydrogels

XG has some drawbacks like bacterial contamination; it was previously mentioned in the limitation of XG section 1.2.1.6. Bacterial contamination reduces the shelf-life of food products and increases the risk of foodborne diseases (FBD) that threaten human health [143, 144]. To improve the antibacterial activity of XG, it can react with antibacterial polymers such as chitosan and polyacrylic acid [145, 146] and an antibacterial agent such as chlorhexidine [147].

Chitosan (Ch) is a modified natural copolymer polysaccharide, and it has a polycationic nature. It is composed of β-(1→ 4) linked to copolymer of glucosamine units and *N*-acetyl glucosamine units (Fig. **9a**). Ch is prepared by deacetylation of the *N*-acetyl glucosamine units of chitin under partial alkaline hydrolysis at high temperatures. The deacetylation of chitin rarely reaches full completion. Ch has different molecular weights ($5X10^4$ Da -$2X10^6$ Da) and degree of deacetylation (DD) (40% - 98%). Ch is widely used in several fields such as biomedical, food additives, antimicrobial agents, pharmaceutical, wastewater treatment, paper, and textiles because Ch has excellent properties such as antimicrobial, antioxidant, biodegradable, biocompatible, non-toxic, and anti-inflammatory properties [147-156].

Poly(acrylic acid) (PAA) is a water-soluble anionic synthetic polymer (Fig. **9b**). PAA is synthesized with a free radical polymerization of acrylic acid [157]. PAA has been used in many applications in different fields: superabsorbent and pharmaceutical preparations, soil-enhancing agents, wastewater treatment, and antibacterial applications [82, 157, 158].

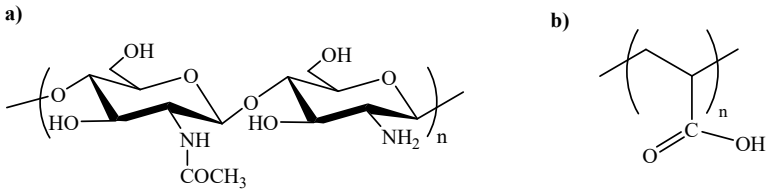

Figure 9: Chemical structure of a) chitosan and b) poly(acrylic acid).

Chlorhexidine (CHX) is a cationic bis-biguanide antimicrobial agent. CHX has a wide-spectrum antimicrobial activity against gram-negative and gram-positive bacteria, yeast, some lipophilic viruses, and dermatophytes because CHX damages the inner (cytoplasmic) membrane that leads to cell lysis and death [147, 159-161]. In addition, CHX is low-toxic against mammalian tissues and has a strong affinity to skin and mucous membrane. Also, it is used in dental treatments for both plaque control and gingival inflammation [147, 159, 161].

Kaith *et al.* [146] reported the synthesis of biodegradable semi-interpenetrating networks (semi-IPN) hydrogels based on grafted copolymerization of XG with acrylic acid (AA) using APS initiator and glutaraldehyde (GA) cross-linking agent. Maximum GY % reached a peak of 2890.03 % when optimum parameters were [APS]= 12.52 $mmolL^{-1}$, [AA]= 4.16 $molL^{-1}$, [GA]= 6.04 $molL^{-1}$, pH= 7.0, microwave power= 90% and grafting reaction time= 90s. The swelling ability of XG hydrogel (XG-g-PAA/GA) was studied at different time intervals, temperatures, pHs, and salt solutions (NaCl, $SrCl_2$, $FeCl_3$, and $SnCl_4$) with varied ionic strength (1,5,10, 15, and 20%). The results showed that XG hydrogels were good sensitive towards both temperatures and pH changes along with the effect of both ionic strength and cationic charges, Na^{+}> Sr^{2+}> Fe^{3+}> Sn^{4+}, on the percentage of swelling. In addition, the biodegradability of semi-IPN hydrogels was studied using the soil burial method, and the data represented that synthesized hydrogel was degraded up to 78.3 % with a degradation rate daily was 1.11 % by weight within 70 days. A biodegradable sample was confirmed with FTIR spectroscopy and SEM micrographs. *Phaseolus vulgaris* plants were chosen to grow in the soil containing the biodegraded sample, and the observations exhibited the absence of harmful end-products from the biodegraded sample. Moreover, the antibacterial activity of synthesized XG hydrogel was evaluated against *Bacillus subtilis* as a Gram-positive bacterium and *Salmonella enteritis* as Gram-negative bacterium using agar well diffusion method in the presence of amoxicillin as a control. The antibacterial activity of the tested sample was evaluated by the diameter of the inhibition zone against the previous two bacteria. The results exhibited resistance of hydrogels to *Bacillus subtilis* and *Salmonella enteritis*, while amoxicillin had good resistance against two bacteria strains. The inhibition zone diameter of hydrogel and amoxicillin against *Bacillus subtilis* was 14.17 mm and 40.56 mm, respectively, and against *Salmonella enteritis* was 13.66 mm and 43.66 mm, respectively.

Kim *et al.* [147] synthesized XG/Ch/ CHX injectable antibacterial hydrogels via the formation of polyelectrolyte complex (PEC) hydrogel between anionic XG and cationic Ch. It was mixed with CHX dihydrochloride and CHX digluconate through electrostatic attractions. XG/Ch/CHX hydrogels were potentially used for acute or chronic periodontitis. XG/Ch PEC microspheres were synthesized by coacervation to increase their both adherent properties and viscosity. Synthesized XG/Ch/CHX hydrogels were characterized with various analysis techniques: SEM and FTIR techniques. The characterization of delivering CHX from XG/Ch/CHX hydrogels was investigated via cytotoxicity, rheological analysis, and antibacterial activity. Cytotoxicity of synthesized hydrogels was studied against human dermal fibroblast (HDF) cell lines with Trypan blue exclusion assay, and the results showed that XG hydrogels were noncytotoxic to HDF cells. While rheological analysis exhibited that hydrogels displayed viscoelastic behavior. In addition, the selective antibacterial activity of CHX hydrogels was evaluated against *Porphyromonas gingivalis* (*P. gingivalis*) by blood-agar plate assay. The results presented that XG/Ch/CHX hydrogels inhibited the growth of *P. gingivalis* compared with XG/Ch PEC (in the absence of CHX).

5. Conclusion

Xanthan gum is considered one of the most interesting polysaccharides in recent years and can be used in different fields thanks to its fabulous features: rheological features, biocompatible, safe-material, biodegradable, and abundance. Conversely, many limitations obstacle the usage of xanthan gum in industry, for instance, bacterial attack, low-surface area, weak mechanical and thermal properties.

In this review, we are interested in discussing the XG modifications like grafted XG, the preparation of 3D hydrogel, and XG nanocomposites-based hydroxyl and carboxylic moieties onto XG chains to improve the properties of XG with outstanding features: good antibacterial assay, safe-material, excellent biocompatible and biodegradable, high specific area, excellent mechanical and thermal stabilities. Additionally, this review shows the updated fields that have been done via modified XG, including wastewater treatment, protein delivery, and designing antibacterial XG derivatives.

References

[1] Kalia S, Sabaa MW, Kango S. Polymer grafting: A versatile means to modify the polysaccharides, Polysaccharide based graft copolymers, Springer 2013; pp. 1-14. https://doi.org/10.1007/978-3-642-36566-9_1

[2] Bansal V, Sharma PK, Sharma N, Pal OP, Malviya R. Applications of chitosan and chitosan derivatives in drug delivery, Advances in Biological Research 2011; 5(1): 28-37.

[3] Goda ES, Abu Elella MH, Gamal H, Hong SE, Yoon KR. Two-Dimensional Nanomaterials as Smart Flame Retardants for Polyurethane, Materials and Chemistry of Flame-Retardant Polyurethanes Volume 1: A Fundamental Approach, ACS Publications 2021; pp. 189-219.

[4] Kumar A, Rao KM, Han SS. Application of xanthan gum as polysaccharide in tissue engineering: A review, Carbohydrate Polymers 2017. https://doi.org/10.1016/j.carbpol.2017.10.009

[5] Singh RS, Kaur N, Rana V, Kennedy JF. Recent insights on applications of pullulan in tissue engineering, Carbohydrate Polymers 2016; 153: 455-462. https://doi.org/10.1016/j.carbpol.2016.07.118

[6] Debele TA, Mekuria SL, Tsai H-C. Polysaccharide based nanogels in the drug delivery system: Application as the carrier of pharmaceutical agents, Materials Science and Engineering: C 2016; 68: 964-981. https://doi.org/10.1016/j.msec.2016.05.121

[7] Zhang N, Wardwell PR, Bader RA. Polysaccharide-based micelles for drug delivery, Pharmaceutics 2013;5(2): 329-352. https://doi.org/10.3390/pharmaceutics5020329

[8] Leung M, Liu C, Koon J, Fung K. Polysaccharide biological response modifiers, Immunology letters 2006; 105(2): 101-114. https://doi.org/10.1016/j.imlet.2006.01.009

[9] Ngwuluka NC, Abu-Thabit NY, Uwaezuoke OJ, Erebor JO, Ilomuanya MO, Mohamed RR, et al. Natural Polymers in Micro-and Nanoencapsulation for Therapeutic and Diagnostic Applications: Part II-Polysaccharides and Proteins, Nano-and Microencapsulation: Techniques and Applications 2021; 55. https://doi.org/10.5772/intechopen.95402

[10] Elella M, Abdel-Aziz MM, Abd El-Ghany NA. Synthesis of a high-performance antimicrobial o-quaternized alginate-a promising potential antimicrobial agent, Cellul Chem Technol Synth 2021; 55: 75-86. https://doi.org/10.35812/CelluloseChemTechnol.2021.55.08

[11] Goda ES, Elella MHA, Sohail M, Singu BS, Pandit B, El Shafey A, et al. N-methylene phosphonic acid chitosan/graphene sheets decorated with silver nanoparticles as green antimicrobial agents, International Journal of Biological Macromolecules 2021; 182: 680-688. https://doi.org/10.1016/j.ijbiomac.2021.04.024

[12] Goda ES, Elella MHA, Hong SE, Pandit B, Yoon KR, Gamal H. Smart flame retardant coating containing carboxymethyl chitosan nanoparticles decorated graphene for obtaining multifunctional textiles, Cellulose 2021; 28(8): 5087-5105. https://doi.org/10.1007/s10570-021-03833-7

[13] Elella MHA, Goda ES, Yoon KR, Hong SE, Morsy MS, Sadak RA, et al. Novel vapor polymerization for integrating flame retardant textile with multifunctional properties, Composites Communications 2021; 24: 100614. https://doi.org/10.1016/j.coco.2020.100614

[14] Miller T, Goude MC, McDevitt TC, Temenoff JS. Molecular engineering of glycosaminoglycan chemistry for biomolecule delivery, Acta biomaterialia 2014; 10(4): 1705-1719. https://doi.org/10.1016/j.actbio.2013.09.039

[15] Drogoz A, David L, Rochas C, Domard A, Delair T. Polyelectrolyte complexes from polysaccharides: formation and stoichiometry monitoring, Langmuir 2007; 23(22): 10950-10958. https://doi.org/10.1021/la7008545

[16] Posocco B, Dreussi E, De Santa J, Toffoli G, Abrami M, Musiani F, et al. Polysaccharides for the delivery of antitumor drugs, Materials 2015; 8(5): 2569-2615. https://doi.org/10.3390/ma8052569

[17] Elella MHA, Mohamed RR, Sabaa MW. Synthesis of novel grafted hyaluronic acid with antitumor activity, Carbohydrate polymers 2018; 189: 107-114. https://doi.org/10.1016/j.carbpol.2018.02.004

[18] Kumbar S, Toti U, Deng M, James R, Laurencin C, Aravamudhan A, et al. Novel mechanically competent polysaccharide scaffolds for bone tissue engineering, Biomedical Materials 2011; 6(6): 065005. https://doi.org/10.1088/1748-6041/6/6/065005

[19] Malafaya PB, Silva GA, Reis RL. Natural-origin polymers as carriers and scaffolds for biomolecules and cell delivery in tissue engineering applications, Advanced drug delivery reviews 2007; 59(4-5): 207-233. https://doi.org/10.1016/j.addr.2007.03.012

[20] Shelke NB, James R, Laurencin CT, Kumbar SG. Polysaccharide biomaterials for drug delivery and regenerative engineering, Polymers for Advanced Technologies 2014; 25(5): 448-460. https://doi.org/10.1002/pat.3266

[21] Zohuriaan-Mehr M, Pourjavadi A. New polysaccharide-g-polyacrylonitrile copolymers: synthesis and thermal characterization, Polymers for Advanced Technologies 2003; 14(7): 508-516. https://doi.org/10.1002/pat.362

[22] Pandit B, Goda ES, Elella MHA, Ur-Rehman A, Hong SE, Rondiya SR, et al. One-pot hydrothermal preparation of hierarchical manganese oxide nanorods for high-performance symmetric supercapacitors, Journal of Energy Chemistry 2022; 65: 116-126. https://doi.org/10.1016/j.jechem.2021.05.028

[23] Kumar R, Srivastava A, Behari K. Synthesis and characterization of polysaccharide based graft copolymer by using potassium peroxymonosulphate/ascorbic acid as an efficient redox initiator in inert atmosphere, Journal of applied polymer science 2009; 112(3): 1407-1415. https://doi.org/10.1002/app.29495

[24] Elella MHA, Sabaa M, Hanna DH, Abdel-Aziz MM, Mohamed RR. Antimicrobial pH-sensitive protein carrier based on modified xanthan gum, Journal of Drug Delivery Science and Technology 2020; 57: 101673. https://doi.org/10.1016/j.jddst.2020.101673

[25] Katzbauer B. Properties and applications of xanthan gum, Polymer degradation and stability 1998; 59(1-3): 81-84. https://doi.org/10.1016/S0141-3910(97)00180-8

[26] Jeanes A, Pittsley J, Senti F. Polysaccharide B-1459: a new hydrocolloid polyelectrolyte produced from glucose by bacterial fermentation, Journal of applied polymer science 1961; 5(17): 519-526. https://doi.org/10.1002/app.1961.070051704

[27] Margaritis A, Zajic JE. Mixing, mass transfer, and scale-up of polysaccharide fermentations, Biotechnology and Bioengineering 1978; 20(7): 939-1001. https://doi.org/10.1002/bit.260200702

[28] Garcıa-Ochoa F, Santos V, Casas J, Gomez E. Xanthan gum: production, recovery, and properties, Biotechnology advances 2000; 18(7): 549-579. https://doi.org/10.1016/S0734-9750(00)00050-1

[29] Kennedy JF, Bradshaw I. Production, properties and applications of xanthan, Progress in industrial microbiology 1984.

[30] Habibi H, Khosravi-Darani K. Effective variables on production and structure of xanthan gum and its food applications: A review, Biocatalysis and Agricultural Biotechnology 2017; 10: 130-140. https://doi.org/10.1016/j.bcab.2017.02.013

[31] Ghashghaei T, Soudi MR, Hoseinkhani S. Optimization of xanthan gum production from grape juice concentrate using Plackett-Burman design and response surface methodology, Applied Food Biotechnology 2016; 3(1): 15-23.

[32] Elella MHA, Goda ES, Gab-Allah MA, Hong SE, Pandit B, Lee S, et al. Xanthan gum-derived materials for applications in environment and eco-friendly materials: A review, Journal of Environmental Chemical Engineering 2021; 9(1): 104702. https://doi.org/10.1016/j.jece.2020.104702

[33] Faria S, de Oliveira Petkowicz CL, de Morais SAL, Terrones MGH, de Resende MM, de França FP, et al. Characterization of xanthan gum produced from sugar cane broth, Carbohydrate Polymers 2011; 86(2): 469-476. https://doi.org/10.1016/j.carbpol.2011.04.063

[34] Jansson P-E, Kenne L, Lindberg B. Structure of the extracellular polysaccharide from Xanthomonas campestris, Carbohydrate Research 1975; 45(1): 275-282. https://doi.org/10.1016/S0008-6215(00)85885-1

[35] Abbaszadeh A, Lad M, Janin M, Morris G, MacNaughtan W, Sworn G, et al. A novel approach to the determination of the pyruvate and acetate distribution in xanthan, Food Hydrocolloids 2015; 44: 162-171. https://doi.org/10.1016/j.foodhyd.2014.08.014

[36] Wang Z, Wu J, Zhu L, Zhan X. Characterization of xanthan gum produced from glycerol by a mutant strain Xanthomonas campestris CCTCC M2015714, Carbohydrate Polymers 2017; 157: 521-526. https://doi.org/10.1016/j.carbpol.2016.10.033

[37] Elella MHA, Goda ES, Abdallah HM, Shalan AE, Gamal H, Yoon KR. Innovative bactericidal adsorbents containing modified xanthan gum/montmorillonite nanocomposites for wastewater treatment, International Journal of Biological Macromolecules 2021; 167: 1113-1125. https://doi.org/10.1016/j.ijbiomac.2020.11.065

[38] Cadmus M, Rogovin S, Burton K, Pittsley J, Knutson C, Jeanes A. Colonial variation in Xanthomonas campestris NRRL B-1459 and characterization of the polysaccharide from a variant strain, Canadian Journal of Microbiology 1976; 22(7): 942-948. https://doi.org/10.1139/m76-136

[39] Sutherland I. Xanthomonas polysaccharides-improved methods for their comparison, Carbohydrate Polymers 1981; 1(2): 107-115. https://doi.org/10.1016/0144-8617(81)90003-5

[40] Tait M, Sutherland I, Clarke-Sturman A. Effect of growth conditions on the production, composition and viscosity of Xanthomonas campestris exopolysaccharide, Microbiology 1986; 132(6): 1483-1492. https://doi.org/10.1099/00221287-132-6-1483

[41] Moorhouse R, Walkinshaw M, Arnott S. Xanthan Gum Molecular Conformation and Interactions, ACS Publications 1977. https://doi.org/10.1021/bk-1977-0045.ch007

[42] Cheetham NW, Mashimba EN. Proton and carbon-13 NMR studies on xanthan derivatives, Carbohydrate Polymers 1992; 17(2): 127-136. https://doi.org/10.1016/0144-8617(92)90106-Z

[43] Holzwarth G. Conformation of the extracellular polysaccharide of Xanthomonas campestris, Biochemistry 1976; 15(19): 4333-4339. https://doi.org/10.1021/bi00664a030

[44] Fiume MM, Heldreth B, Bergfeld WF, Belsito DV, Hill RA, Klaassen CD, et al. Safety assessment of microbial polysaccharide gums as used in cosmetics, International journal of toxicology 2016; 35(1_suppl): 5S-49S. https://doi.org/10.1177/1091581816651606

[45] Farhadi GB, Khosravi-Darani K, Nejad BN. Enhancement of Xanthan production on date extract using response surface methodology, Asian J Chem 2012; 24: 3887-3890.

[46] Niknezhad SV, Asadollahi MA, Zamani A, Biria D. Production of xanthan gum by free and immobilized cells of Xanthomonas campestris and Xanthomonas pelargonii, International journal of biological macromolecules 2016; 82: 751-756. https://doi.org/10.1016/j.ijbiomac.2015.10.065

[47] Leela JK, Sharma G. Studies on xanthan production from Xanthomonas campestris, Bioprocess Engineering 2000; 23(6): 687-689. https://doi.org/10.1007/s004499900054

[48] Benny IS, Gunasekar V, Ponnusami V. Review on application of xanthan gum in drug delivery, Int J PharmTech Res 2014; 6(4): 1322-1326.

[49] Bejenariu A, Popa M, Dulong V, Picton L, Le Cerf D. Trisodium trimetaphosphate cross-linked xanthan networks: synthesis, swelling, loading and releasing behaviour, Polymer Bulletin 2009; 62(4): 525-538. https://doi.org/10.1007/s00289-008-0033-8

[50] Petri DF. Xanthan gum: A versatile biopolymer for biomedical and technological applications, Journal of Applied Polymer Science 2015; 132(23). https://doi.org/10.1002/app.42035

[51] Rinaudo M, Milas M. Enzymic hydrolysis of the bacterial polysaccharide xanthan by cellulase, International Journal of Biological Macromolecules 1980; 2(1): 45-48. https://doi.org/10.1016/0141-8130(80)90009-4

[52] Badwaik HR, Kumar Giri T, Nakhate KT, Kashyap P, Tripathi DK. Xanthan gum and its derivatives as a potential bio-polymeric carrier for drug delivery system, Current Drug Delivery 2013; 10(5): 587-600. https://doi.org/10.2174/1567201811310050010

[53] Krstonošić V, Dokić L, Dokić P, Dapčević T. Effects of xanthan gum on physicochemical properties and stability of corn oil-in-water emulsions stabilized by polyoxyethylene (20) sorbitan monooleate, Food Hydrocolloids 2009; 23(8): 2212-2218. https://doi.org/10.1016/j.foodhyd.2009.05.003

[54] Comba S, Sethi R. Stabilization of highly concentrated suspensions of iron nanoparticles using shear-thinning gels of xanthan gum, Water Research 2009; 43(15): 3717-3726. https://doi.org/10.1016/j.watres.2009.05.046

[55] Takeuchi A, Kamiryou Y, Yamada H, Eto M, Shibata K, Haruna K, et al. Oral administration of xanthan gum enhances antitumor activity through Toll-like receptor 4, International Immunopharmacology 2009; 9(13-14): 1562-1567. https://doi.org/10.1016/j.intimp.2009.09.012

[56] Rosalam S, England R. Review of xanthan gum production from unmodified starches by Xanthomonas comprestris sp, Enzyme and Microbial Technology 2006; 39(2): 197-207. https://doi.org/10.1016/j.enzmictec.2005.10.019

[57] Palaniraj A, Jayaraman V. Production, recovery and applications of xanthan gum by Xanthomonas campestris, Journal of Food Engineering 2011; 106(1): 1-12. https://doi.org/10.1016/j.jfoodeng.2011.03.035

[58] Chang I, Im J, Prasidhi AK, Cho G-C. Effects of Xanthan gum biopolymer on soil strengthening, Construction and Building Materials 2015; 74: 65-72. https://doi.org/10.1016/j.conbuildmat.2014.10.026

[59] Srivastava A, Mishra DK, Tripathy J, Behari K. One pot synthesis of xanthan gum-g-N-vinyl-2-pyrrolidone and study of their metal ion sorption behavior and water swelling property, Journal of applied polymer science 2009; 111(6): 2872-2880. https://doi.org/10.1002/app.29186

[60] Su L, Ji W, Lan W, Dong X. Chemical modification of xanthan gum to increase dissolution rate, Carbohydrate Polymers 2003; 53(4): 497-499. https://doi.org/10.1016/S0144-8617(02)00287-4

[61] Pal S, Das R. Polysaccharide-based graft copolymers for biomedical applications, Polysaccharide Based Graft Copolymers, Springer 2013; pp. 325-345. https://doi.org/10.1007/978-3-642-36566-9_9

[62] Kumar A, Singh K, Ahuja M. Xanthan-g-poly (acrylamide): microwave-assisted synthesis, characterization and in vitro release behavior, Carbohydrate Polymers 2009; 76(2): 261-267. https://doi.org/10.1016/j.carbpol.2008.10.014

[63] Li YF, Ha YM, Tao LR, Li YJ, Wang F. Preparation of xanthan gum-gN-vinylpyrrolidone by radiation and adsorption property of phenol and polyphenol, Advanced Materials Research, Trans Tech Publ, 2011; pp. 2694-2700. https://doi.org/10.4028/www.scientific.net/AMR.236-238.2694

[64] Caner H, Yilmaz E, Yilmaz O. Synthesis, characterization and antibacterial activity of poly (N-vinylimidazole) grafted chitosan, Carbohydrate Polymers 2007; 69(2): 318-325. https://doi.org/10.1016/j.carbpol.2006.10.008

[65] Badwaik HR, Sakure K, Alexander A, Dhongade H, Tripathi DK. Synthesis and characterisation of poly (acryalamide) grafted carboxymethyl xanthan gum copolymer, International Journal of Biological Macromolecules 2016; 85: 361-369. https://doi.org/10.1016/j.ijbiomac.2016.01.014

[66] Elella MHA, Mohamed RR, Abd ElHafeez E, Sabaa MW. Synthesis of novel biodegradable antibacterial grafted xanthan gum, Carbohydrate Polymers 2017; 173: 305-311. https://doi.org/10.1016/j.carbpol.2017.05.058

[67] Pandey PK, Banerjee J, Taunk K, Behari K. Graft copolymerization of acrylic acid onto xanthum gum using a potassium monopersulfate/Fe2+ redox pair, Journal of Applied Polymer Science 2003; 89(5): 1341-1346. https://doi.org/10.1002/app.12302

[68] Sand A, Yadav M, Behari K. Graft copolymerization of 2-Acrylamidoglycolic acid on to xanthan gum and study of its physicochemical properties, Carbohydrate Polymers 2010; 81(3): 626-632. https://doi.org/10.1016/j.carbpol.2010.03.022

[69] Pandey S, Mishra SB. Graft copolymerization of ethylacrylate onto xanthan gum, using potassium peroxydisulfate as an initiator, International Journal of Biological Macromolecules 2011; 49(4): 527-535. https://doi.org/10.1016/j.ijbiomac.2011.06.005

[70] Mundargi RC, Patil SA, Aminabhavi TM. Evaluation of acrylamide-grafted-xanthan gum copolymer matrix tablets for oral controlled delivery of antihypertensive drugs, Carbohydrate Polymers 2007; 69(1): 130-141. https://doi.org/10.1016/j.carbpol.2006.09.007

[71] Jayaramudu T, Ko H-U, Zhai L, Li Y, Kim J. Preparation and characterization of hydrogels from polyvinyl alcohol and cellulose and their electroactive behavior, Soft Materials 2017; 15(1): 64-72. https://doi.org/10.1080/1539445X.2016.1246458

[72] Peppas NA, Khare AR. Preparation, structure and diffusional behavior of hydrogels in controlled release, Advanced Drug Delivery Reviews 1993;11(1-2): 1-35. https://doi.org/10.1016/0169-409X(93)90025-Y

[73] Pekel N, Güven O. Synthesis and characterization of poly (N-vinyl imidazole) hydrogels cross-linked by gamma irradiation, Polymer International 2002; 51(12): 1404-1410. https://doi.org/10.1002/pi.1065

[74] Sharma G, Thakur B, Naushad M, Kumar A, Stadler FJ, Alfadul SM, et al. Applications of nanocomposite hydrogels for biomedical engineering and environmental protection, Environmental Chemistry Letters 2017; 1-34. https://doi.org/10.1007/s10311-017-0671-x

[75] Ahmed EM. Hydrogel: Preparation, characterization, and applications: A review, Journal of Advanced Research 2015; 6(2): 105-121. https://doi.org/10.1016/j.jare.2013.07.006

[76] Brannon-Peppas L, Peppas NA. Equilibrium swelling behavior of pH-sensitive hydrogels, Chemical Engineering Science 1991; 46(3): 715-722. https://doi.org/10.1016/0009-2509(91)80177-Z

[77] Liu K-H, Liu T-Y, Chen S-Y, Liu D-M. Drug release behavior of chitosan-montmorillonite nanocomposite hydrogels following electrostimulation, Acta Biomaterialia 2008; 4(4): 1038-1045. https://doi.org/10.1016/j.actbio.2008.01.012

[78] Roy D, Cambre JN, Sumerlin BS. Future perspectives and recent advances in stimuli-responsive materials, Progress in Polymer Science 2010; 35(1-2): 278-301. https://doi.org/10.1016/j.progpolymsci.2009.10.008

[79] Kamath KR, Park K. Biodegradable hydrogels in drug delivery, Advanced drug delivery reviews 1993; 11(1-2): 59-84. https://doi.org/10.1016/0169-409X(93)90027-2

[80] Manjula B, Reddy AB, Jayaramudu T, Sadiku E, Owonubi S, Agboola O, et al. Hydrogels and its Nanocomposites from Renewable Resources: Biotechnological and Biomedical Applications, Handbook of Composites from Renewable Materials, Nanocomposites: Science and Fundamentals 2017; 7: 67. https://doi.org/10.1002/9781119441632.ch127

[81] Tanaka Y, Gong JP, Osada Y. Novel hydrogels with excellent mechanical performance, Progress in Polymer science 2005; 30(1): 1-9. https://doi.org/10.1016/j.progpolymsci.2004.11.003

[82] Bekin S, Sarmad S, Gürkan K, Keçeli G, Gürdağ G. Synthesis, characterization and bending behavior of electroresponsive sodium alginate/poly (acrylic acid) interpenetrating network films under an electric field stimulus, Sensors and Actuators B: Chemical 2014; 202: 878-892. https://doi.org/10.1016/j.snb.2014.06.051

[83] Mellati A, Dai S, Bi J, Jin B, Zhang H. A biodegradable thermosensitive hydrogel with tuneable properties for mimicking three-dimensional microenvironments of stem cells, RSC Advances 2014; 4(109): 63951-63961. https://doi.org/10.1039/C4RA12215A

[84] Discher DE, Janmey P, Wang Y-l. Tissue cells feel and respond to the stiffness of their substrate, Science 2005; 310(5751): 1139-1143. https://doi.org/10.1126/science.1116995

[85] Giri T, Choudhary C, Alexander A. Sustained release of diltiazem hydrochloride from cross-linked biodegradable IPN hydrogel beads of pectin and modified xanthan gum, Indian journal of pharmaceutical sciences 2013; 75(6): 619.

[86] Raveendran RL, Devaki SJ, Nampoothiri KM. Facile strategy for the development of polyglucopyranose-silver hydrogel/films for antimicrobial applications, RSC Advances 2016; 6(114): 113648-113656. https://doi.org/10.1039/C6RA21632C

[87] Pekel N, Güven O. Separation of heavy metal ions by complexation on poly (N-vinyl imidazole) hydrogels, Polymer Bulletin 2004; 51(4): 307-314. https://doi.org/10.1007/s00289-004-0224-x

[88] Sadeghi M, Soleimani F. Synthesis and characterization superabsorbent hydrogelsfor oral drug delivery systems, International Journal of Chemical Engineering and Applications 2011; 2(5): 314. https://doi.org/10.7763/IJCEA.2011.V2.125

[89] Gils PS, Ray D, Sahoo PK. Characteristics of xanthan gum-based biodegradable superporous hydrogel, International journal of biological macromolecules 2009; 45(4): 364-371. https://doi.org/10.1016/j.ijbiomac.2009.07.007

[90] Shalviri A, Liu Q, Abdekhodaie MJ, Wu XY. Novel modified starch-xanthan gum hydrogels for controlled drug delivery: Synthesis and characterization, Carbohydrate Polymers 2010; 79(4): 898-907. https://doi.org/10.1016/j.carbpol.2009.10.016

[91] Argin S, Kofinas P, Lo YM. The cell release kinetics and the swelling behavior of physically cross-linked xanthan-chitosan hydrogels in simulated gastrointestinal conditions, Food Hydrocolloids 2014; 40: 138-144. https://doi.org/10.1016/j.foodhyd.2014.02.018

[92] Laemmli UK. Cleavage of structural proteins during the assembly of the head of bacteriophage T4, Nature 1970; 227(5259): 680. https://doi.org/10.1038/227680a0

[93] He Y, Yeung ES. Rapid determination of protein molecular weight by the Ferguson method and multiplexed capillary electrophoresis, Journal of Proteome Research 2002; 1(3): 273-277. https://doi.org/10.1021/pr025507i

[94] Yu Z, Yu M, Zhang Z, Hong G, Xiong Q. Bovine serum albumin nanoparticles as controlled release carrier for local drug delivery to the inner ear, Nanoscale Research Letters 2014; 9(1): 343. https://doi.org/10.1186/1556-276X-9-343

[95] Bueno VB, Petri DFS. Xanthan hydrogel films: Molecular conformation, charge density and protein carriers, Carbohydrate Polymers 2014; 101: 897-904. https://doi.org/10.1016/j.carbpol.2013.10.039

[96] Raoufinia R, Mota A, Keyhanvar N, Safari F, Shamekhi S, Abdolalizadeh J. Overview of albumin and its purification methods, Advanced Pharmaceutical Bulletin 2016; 6(4): 495. https://doi.org/10.15171/apb.2016.063

[97] Maiti S, Ray S, Mandal B, Sarkar S, Sa B. Carboxymethyl xanthan microparticles as a carrier for protein delivery, Journal of Microencapsulation 2007; 24(8): 743-756. https://doi.org/10.1080/02652040701647300

[98] Sabaa MW, Hanna DH, Elella MHA, Mohamed RR. Encapsulation of bovine serum albumin within novel xanthan gum based hydrogel for protein delivery, Materials Science and Engineering: C 2019; 94: 1044-1055. https://doi.org/10.1016/j.msec.2018.10.040

[99] Abu Elella MH, Hanna DH, Mohamed RR, Sabaa MW. Synthesis of xanthan gum/trimethyl chitosan interpolyelectrolyte complex as pH-sensitive protein carrier, Polymer Bulletin 2021; 1-22. https://doi.org/10.1007/s00289-021-03656-3

[100] Liu B, Chen X, Zheng H, Wang Y, Sun Y, Zhao C, et al. Rapid and efficient removal of heavy metal and cationic dye by carboxylate-rich magnetic chitosan flocculants: Role of ionic groups, Carbohydrate Polymers 2018; 181: 327-336. https://doi.org/10.1016/j.carbpol.2017.10.089

[101] Kumari HJ, Krishnamoorthy P, Arumugam T, Radhakrishnan S, Vasudevan D. An efficient removal of crystal violet dye from waste water by adsorption onto TLAC/Chitosan composite: A novel low cost adsorbent, International Journal of Biological Macromolecules 2017; 96: 324-333. https://doi.org/10.1016/j.ijbiomac.2016.11.077

[102] Abu-Thabit NY, Uwaezuoke OJ, Elella MHA. Superhydrophobic nanohybrid sponges for separation of oil/water mixtures, Chemosphere 2022; 133644. https://doi.org/10.1016/j.chemosphere.2022.133644

[103] Robinson T, McMullan G, Marchant R, Nigam P. Remediation of dyes in textile effluent: a critical review on current treatment technologies with a proposed alternative, Bioresource technology 2001; 77(3): 247-255. https://doi.org/10.1016/S0960-8524(00)00080-8

[104] Thakur S, Arotiba O. Synthesis, characterization and adsorption studies of an acrylic acid-grafted sodium alginate-based TiO2 hydrogel nanocomposite, Adsorption Science & Technology 2018; 36(1-2): 458-477. https://doi.org/10.1177/0263617417700636

[105] Mittal H, Parashar V, Mishra S, Mishra A. Fe3O4 MNPs and gum xanthan based hydrogels nanocomposites for the efficient capture of malachite green from aqueous solution, Chemical Engineering Journal 2014; 255: 471-482. https://doi.org/10.1016/j.cej.2014.04.098

[106] Hu F, Fang C, Wang Z, Liu C, Zhu B, Zhu L. Poly (N-vinyl imidazole) gel composite porous membranes for rapid separation of dyes through permeating adsorption, Separation and Purification Technology 2017; 188: 1-10. https://doi.org/10.1016/j.seppur.2017.06.024

[107] Mittal H, Kumar V, Ray SS. Adsorption of methyl violet from aqueous solution using gum xanthan/Fe3O4 based nanocomposite hydrogel, International Journal of Biological Macromolecules 2016; 89: 1-11. https://doi.org/10.1016/j.ijbiomac.2016.04.050

[108] Kumari K, Abraham TE. Biosorption of anionic textile dyes by nonviable biomass of fungi and yeast, Bioresource Technology 2007; 98(9): 1704-1710. https://doi.org/10.1016/j.biortech.2006.07.030

[109] Martins LR, Rodrigues JAV, Adarme OFH, Melo TMS, Gurgel LVA, Gil LF. Optimization of cellulose and sugarcane bagasse oxidation: Application for adsorptive removal of crystal violet and auramine-O from aqueous solution, Journal of Colloid and Interface Science 2017; 494: 223-241. https://doi.org/10.1016/j.jcis.2017.01.085

[110] Crini G. Non-conventional low-cost adsorbents for dye removal: a review, Bioresource Technology 2006; 97(9): 1061-1085. https://doi.org/10.1016/j.biortech.2005.05.001

[111] Tahir S, Rauf N. Removal of a cationic dye from aqueous solutions by adsorption onto bentonite clay, Chemosphere 2006; 63(11): 1842-1848. https://doi.org/10.1016/j.chemosphere.2005.10.033

[112] Bajpai SK, Jain A. Equilibrium and thermodynamic studies for adsorption of crystal violet onto spent tea leaves (STL), Water 2012; 4: 52-71.

[113] Mani S, Bharagava RN. Exposure to crystal violet, its toxic, genotoxic and carcinogenic effects on environment and its degradation and detoxification for environmental safety, Reviews of Environmental Contamination and Toxicology Springer 2016; 237: pp. 71-104. https://doi.org/10.1007/978-3-319-23573-8_4

[114] Wang Y, Liao K, Huang X, Yuan D. Simultaneous determination of malachite green, crystal violet and their leuco-metabolites in aquaculture water samples using monolithic fiber-based solid-phase microextraction coupled with high performance liquid chromatography, Analytical Methods 2015; 7(19): 8138-8145. https://doi.org/10.1039/C5AY01611H

[115] Lee JB, Yun Kim H, Mi Jang Y, Young Song J, Min Woo S, Sun Park M, et al. Determination of malachite green and crystal violet in processed fish products, Food Additives and Contaminants 2010; 27(7): 953-961. https://doi.org/10.1080/19440041003705839

[116] Abu Elella MH, ElHafeez EA, Goda ES, Lee S, Yoon KR. Smart bactericidal filter containing biodegradable polymers for crystal violet dye adsorption, Cellulose 2019; 26(17): 9179-9206. https://doi.org/10.1007/s10570-019-02698-1

[117] Hasan I, Bassi A, Alharbi KH, BinSharfan II, Khan RA, Alslame AJC. Sonophotocatalytic Degradation of Malachite Green by Nanocrystalline Chitosan-Ascorbic Acid@ NiFe2O4 Spinel Ferrite, 2020; 10(12): 1200. https://doi.org/10.3390/coatings10121200

[118] Baeissa EJJOA. Compounds, Photocatalytic degradation of malachite green dye using Au/NaNbO3 Nanoparticles, 2016; 672: 564-570. https://doi.org/10.1016/j.jallcom.2016.02.024

[119] Hasan I, Bhatia D, Walia S, Singh PJGFSD. Removal of malachite green by polyacrylamide-g-chitosan γ-Fe2O3 nanocomposite-an application of central composite design, 2020; 11: 100378. https://doi.org/10.1016/j.gsd.2020.100378

[120] Elella MHA, Aamer N, Mohamed Y, El Nazer HA, Mohamed RR. Innovation of high-performance adsorbent based on modified gelatin for wastewater treatment, Polymer Bulletin 2022; 1-17. https://doi.org/10.1007/s00289-022-04079-4

[121] Ghorai S, Sarkar A, Raoufi M, Panda AB, Schönherr H, Pal S. Enhanced removal of methylene blue and methyl violet dyes from aqueous solution using a nanocomposite of hydrolyzed polyacrylamide grafted xanthan gum and incorporated nanosilica, ACS Applied Materials & Interfaces 2014; 6(7): 4766-4777. https://doi.org/10.1021/am4055657

[122] Ghorai S, Sarkar AK, Panda AB, Pal S. Effective removal of Congo red dye from aqueous solution using modified xanthan gum/silica hybrid nanocomposite as adsorbent, Bioresource technology 2013; 144: 485-491. https://doi.org/10.1016/j.biortech.2013.06.108

[123] Makhado E, Pandey S, Nomngongo P, Ramontja J. Xanthan gum-cl-poly (acrylic acid)/reduced graphene oxide hydrogel nanocomposite as adsorbent for dye removal, 9th Int'l Conf. on Advances in Science, Engineering, Technology & Waste Management 2017; (ASETWM-17): pp. 159-164.

[124] Thakur S, Pandey S, Arotiba OA. Sol-gel derived xanthan gum/silica nanocomposite-a highly efficient cationic dyes adsorbent in aqueous system, International journal of biological macromolecules 2017; 103: 596-604. https://doi.org/10.1016/j.ijbiomac.2017.05.087

[125] Tanzifi M, Esmizadeh E, Bazgir H, Nazari A, Vahidifar A. Adsorption of methylene blue dye from aqueous solution using polyaniline/xanthan gum nanocomposite: kinetic and isotherm studies, J Polym Compos 2019; 7: 17-26.

[126] Hosseini SM, Shahrousvand M, Shojaei S, Khonakdar HA, Asefnejad A, Goodarzi V. Preparation of superabsorbent eco-friendly semi-interpenetrating network based on cross-linked poly acrylic acid/xanthan gum/graphene oxide (PAA/XG/GO): Characterization and dye removal ability, International journal of biological macromolecules 2020; 152: 884-893. https://doi.org/10.1016/j.ijbiomac.2020.02.082

[127] Ahmad R, Mirza A. Green synthesis of Xanthan gum/Methionine-bentonite nanocomposite for sequestering toxic anionic dye, Surfaces and Interfaces 2017; 8: 65-72. https://doi.org/10.1016/j.surfin.2017.05.001

[128] Chen X, Li P, Zeng X, Kang Y, Wang J, Xie H, et al. Efficient adsorption of methylene blue by xanthan gum derivative modified hydroxyapatite, International journal of biological macromolecules 2019. https://doi.org/10.1016/j.ijbiomac.2019.10.145

[129] Sharma J, Kaith BS, Sharma AK, Goel A. Gum xanthan-psyllium-cl-poly (acrylic acid-co-itaconic acid) based adsorbent for effective removal of cationic and anionic dyes: adsorption isotherms, kinetics and thermodynamic studies, Ecotoxicology and Environmental Safety 2018; 149: 150-158. https://doi.org/10.1016/j.ecoenv.2017.11.030

[130] Mittal H, Babu R, Alhassan SM. Utilization of gum xanthan based superporous hydrogels for the effective removal of methyl violet from aqueous solution, International Journal of Biological Macromolecules 2020; 143: 413-423. https://doi.org/10.1016/j.ijbiomac.2019.11.008

[131] Elella MHA, Goda ES, Gamal H, El-Bahy SM, Nour MA, Yoon KR. Green antimicrobial adsorbent containing grafted xanthan gum/SiO2 nanocomposites for malachite green dye, International Journal of Biological Macromolecules 2021; 191: 385-395. https://doi.org/10.1016/j.ijbiomac.2021.09.040

[132] Mohamed RR, Abu Elella MH, Sabaa MW, Saad GR. Synthesis of an efficient adsorbent hydrogel based on biodegradable polymers for removing crystal violet dye from aqueous solution, Cellulose 2018; 25(11): 6513-6529. https://doi.org/10.1007/s10570-018-2014-x

[133] Elella MHA, Sabaa MW, Abd ElHafeez E, Mohamed RR. Crystal violet dye removal using cross-linked grafted xanthan gum, International journal of biological macromolecules 2019; 137: 1086-1101. https://doi.org/10.1016/j.ijbiomac.2019.06.243

[134] Zheng M, Lian F, Xiong Y, Liu B, Zhu Y, Miao S, et al. The synthesis and characterization of a xanthan gum-acrylamide-trimethylolpropane triglycidyl ether hydrogel, Food chemistry 2019; 272: 574-579. https://doi.org/10.1016/j.foodchem.2018.08.083

[135] Pandey N, Shukla S, Singh N. Water purification by polymer nanocomposites: an overview, Nanocomposites 2017; 3(2): 47-66. https://doi.org/10.1080/20550324.2017.1329983

[136] Lim AP, Aris AZ. A review on economically adsorbents on heavy metals removal in water and wastewater, Reviews in Environmental Science and Bio/Technology 2014; 13(2): 163-181. https://doi.org/10.1007/s11157-013-9330-2

[137] Ghorai S, Sinhamahpatra A, Sarkar A, Panda AB, Pal S. Novel biodegradable nanocomposite based on XG-g-PAM/SiO2: application of an efficient adsorbent for Pb2+ ions from aqueous solution, Bioresource Technology 2012; 119: 181-190. https://doi.org/10.1016/j.biortech.2012.05.063

[138] Lai KC, Lee LY, Hiew BYZ, Thangalazhy-Gopakumar S, Gan S. Facile synthesis of xanthan biopolymer integrated 3D hierarchical graphene oxide/titanium dioxide composite for adsorptive lead removal in wastewater, Bioresource technology 2020; 123296. https://doi.org/10.1016/j.biortech.2020.123296

[139] Ahmad R, Mirza A. Application of Xanthan gum/n-acetyl cysteine modified mica bionanocomposite as an adsorbent for the removal of toxic heavy metals, Groundwater for Sustainable Development 2018; 7: 101-108. https://doi.org/10.1016/j.gsd.2018.03.010

[140] Jalali MA, Koohi AD, Sheykhan M. Experimental study of the removal of copper ions using hydrogels of xanthan, 2-acrylamido-2-methyl-1-propane sulfonic acid, montmorillonite: kinetic and equilibrium study, Carbohydrate Polymers 2016; 142: 124-132. https://doi.org/10.1016/j.carbpol.2016.01.033

[141] Zhang S, Xu F, Wang Y, Zhang W, Peng X, Pepe F. Silica modified calcium alginate-xanthan gum hybrid bead composites for the removal and recovery of Pb (II) from aqueous solution, Chemical Engineering Journal 2013; 234: 33-42. https://doi.org/10.1016/j.cej.2013.08.102

[142] Iftekhar S, Srivastava V, Hammouda SB, Sillanpää M. Fabrication of novel metal ion imprinted xanthan gum-layered double hydroxide nanocomposite for adsorption of rare earth elements, Carbohydrate polymers 2018; 194: 274-284. https://doi.org/10.1016/j.carbpol.2018.04.054

[143] Quintavalla S, Vicini L. Antimicrobial food packaging in meat industry, Meat Science 2002; 62(3): 373-380. https://doi.org/10.1016/S0309-1740(02)00121-3

[144] Gurbuz O, Sahan Y, Kara A, Osman B. In-Vitro Characterization of Antimicrobial Effect of Polyvinylimidazole, Hacettepe Journal of Biology and Chemistry 2009; 37: 353-7.

[145] Zheng L-Y, Zhu J-F. Study on antimicrobial activity of chitosan with different molecular weights, Carbohydrate Polymers 2003; 54(4): 527-530. https://doi.org/10.1016/j.carbpol.2003.07.009

[146] Kaith B, Jindal R, Kumari M, Kaur M. Biodegradable-stimuli sensitive xanthan gum based hydrogel: evaluation of antibacterial activity and controlled agro-chemical release, Reactive and Functional Polymers 2017; 120: 1-13. https://doi.org/10.1016/j.reactfunctpolym.2017.08.012

[147] Kim J, Hwang J, Seo Y, Jo Y, Son J, Choi J. Engineered chitosan-xanthan gum biopolymers effectively adhere to cells and readily release incorporated antiseptic molecules in a sustained manner, Journal of Industrial and Engineering Chemistry 2017; 46: 68-79. https://doi.org/10.1016/j.jiec.2016.10.017

[148] Swatantra K, Awani R, Satyawan S. Chitosan. A platform for targeted drug delivery, Int J of pharm tech research 2010; 2: 2271-2282.

[149] Ilium L. Chitosan and its use as a pharmaceutical excipient, Pharmaceutical Research 1998; 15(9): 1326-1331. https://doi.org/10.1023/A:1011929016601

[150] Badwan AA, Rashid I, Al Omari MM, Darras FH. Chitin and chitosan as direct compression excipients in pharmaceutical applications, Marine Drugs 2015; 13(3): 1519-1547. https://doi.org/10.3390/md13031519

[151] Duttagupta DS, Jadhav VM, Kadam VJ. Chitosan: a propitious biopolymer for drug delivery, Current Drug Delivery 2015; 12(4): 369-381. https://doi.org/10.2174/1567201812666150310151657

[152] Ariful Islam M, Park T-E, Reesor E, Cherukula K, Hasan A, Firdous J, et al. Mucoadhesive chitosan derivatives as novel drug carriers, Current pharmaceutical design 2015; 21(29): 4285-4309. https://doi.org/10.2174/1381612821666150901103819

[153] Cheung RCF, Ng TB, Wong JH, Chan WY. Chitosan: an update on potential biomedical and pharmaceutical applications, Marine drugs 2015; 13(8): 5156-5186. https://doi.org/10.3390/md13085156

[154] Ferrero F, Periolatto M. Antimicrobial finish of textiles by chitosan UV-curing, Journal of Nanoscience and Nanotechnology 2012; 12(6): 4803-4810. https://doi.org/10.1166/jnn.2012.4902

[155] Despond S, Espuche E, Cartier N, Domard A. Barrier properties of paper-chitosan and paper-chitosan-carnauba wax films, Journal of applied polymer science 2005; 98(2): 704-710. https://doi.org/10.1002/app.21754

[156] Elella MHA, Shalan AE, Sabaa MW, Mohamed RR. One-pot green synthesis of antimicrobial chitosan derivative nanocomposites to control foodborne pathogens, RSC Advances 2022; 12(2): 1095-1104. https://doi.org/10.1039/D1RA07070C

[157] Dai J, Yan H, Yang H, Cheng R. Simple method for preparation of chitosan/poly (acrylic acid) blending hydrogel beads and adsorption of copper (II) from aqueous solutions, Chemical Engineering Journal 2010; 165(1): 240-249. https://doi.org/10.1016/j.cej.2010.09.024

[158] Ortega-Ortiz H, Gutiérrez-Rodríguez B, Cadenas-Pliego G, Jimenez LI. Antibacterial activity of chitosan and the interpolyelectrolyte complexes of poly (acrylic acid)-chitosan, Brazilian Archives of Biology and Technology 2010; 53(3): 623-628. https://doi.org/10.1590/S1516-89132010000300016

[159] Jones CG. Chlorhexidine: is it still the gold standard?, Periodontology 1997; 15(1): 55-62. https://doi.org/10.1111/j.1600-0757.1997.tb00105.x

[160] Huynh TTN, Padois K, Sonvico F, Rossi A, Zani F, Pirot F, et al. Characterization of a polyurethane-based controlled release system for local delivery of chlorhexidine diacetate, European Journal of Pharmaceutics and Biopharmaceutics 2010; 74(2): 255-264. https://doi.org/10.1016/j.ejpb.2009.11.002

[161] Paolantonio M, D'angelo M, Grassi RF, Perinetti G, Piccolomini R, Pizzo G, et al. Clinical and microbiologic effects of subgingival controlled-release delivery of chlorhexidine chip in the treatment of periodontitis: a multicenter study, Journal of periodontology 2008; 79(2): 271-282. https://doi.org/10.1902/jop.2008.070308